Project Number: 1504

YEAST ATF2 GENE EXPRESSION AND WINE AROMA:

A WINE PRODUCTION AND AGENT-BASED MODELING APPROACH

A Major Qualifying Project Report:

Submitted to the Faculty

Of the

WORCESTER POLYTECHNIC INSTITUTE

In partial fulfillment of the requirements for the

Degree of Bachelor of Science

By

Tete Zhang

Date: 4/28/2016

Approved:

_____

Prof. Tanja Dominko, Advisor

_____

Prof. Elizabeth Ryder, Advisor

TABLE OF CONTENTS

ACKNOWLEDGEMENTS iii
LIST OF FIGURES iv
LIST OF TABLES v
ABSTRACT vi
1. BACKGROUND 1
1.1 Wine Profile 1
1.2 Wine Aroma 1
1.3 Biosynthetic Pathways in Yeast Fermentation 2
1.4 Wine Must 4
1.5 The Influence of Environmental Condition Change to Wine Fermentation 5
1.6 Bioinformatics in Wine Research 7
1.7 Virtual Wine Fermentation Simulation 7
2. MATERIALS AND METHODS 9
2.1 Fermentation Set Up 9
2.2 Sugar Content Monitoring 15
2.3 Ester Level Detection and Measurement 15
2.4 RNA Extraction 17
2.5 RT-PCR and Agarose Gel Electrophoresis 17
2.6 Bradford Assay 19
2.7 Bioinformatics 20
2.8 Wine: Simulation Overview, Design Concepts, and Details (ODD) 21
3. RESULTS 26
3.1 Wine Tasting Panel Evaluation 27
3.2 GC-MS 31
3.3 RT-PCR 33
3.4 Bradford Assay 35
3.5 Bioinformatics 36
3.6 NetLogo Wine Fermentation Simulation 42
4. DISCUSSION 50
4.1 Evaluation of Fermentation Regarding ATF2 Gene Transcription and Translation 50
4.2 Evaluation of Fermentation Regarding Market Value and Precise Ester Content 52
4.3 NetLogo Simulation and Wine Fermentation 53
4.4 AAT Enzyme in Other Yeast Strains 54
5. CONCLUSIONS AND FUTURE STEPS 56
REFERENCES 57
APPENDIX A 61
APPENDIX B 62
APPENDIX C 64

ACKNOWLEDGEMENTS

I would like to express my special thanks to:

Dr. Tanja Dominko for advising the biotechnology section of the project;

Dr. Elizabeth Ryder for advising the bioinformatics section of the project;

WPI IGSD for setting up the Slovenia MQP site;

Wine Research Center of University of Nova Gorica for providing research facilities and resources;

Dr. Melita Sternad Lemut for her kind advisory of the wine production process and organization of the tasting panel;

Dr. Drew Brodeur for his kind advisory of the GC-MS analysis;

Dr. Tanja Bele for her kind advisory of the wet lab assays;

Dr. Sofia Dashko for her kind advisory of the fermentation set up;

Sunny Sang Nguyen for her kind support throughout the year.

LIST OF FIGURES

Figure 1: Major Biochemical Pathways in Yeast Fermentation 2
Figure 2: Fermentation Flask Final Set Up 13
Figure 3: Incubator Set at 35°C 14
Figure 4: Incubator Set at 15°C 14
Figure 5: Scores of Citrus Fruit Aroma (Sample 1-9) 28
Figure 6: Scores of Apple/Pear Fruit Aroma (Sample 1-9) 28
Figure 7: Scores of Banana Fruit Aroma (Sample 1-9) 29
Figure 8: Scores of Berry Fruit Aroma (Sample 1-9) 29
Figure 9: Scores of Flowery Aroma (Sample 1-9) 29
Figure 10: Scores of Spice Aroma (Sample 1-9) 30
Figure 11: Scores of Honey Aroma (Sample 1-9) 30
Figure 12: Gas Chromatography - Sample 8, with the phenylethyl alcohol peak pointed out by the red arrow 32
Figure 13: Gas Chromatography - Grape Must Fermentation, with ethyl acetate pointed out by red arrow 33
Figure 14: RT-PCR Product Agarose Gel Electrophoresis 34
Figure 15: Comparison of the AAT protein sequence in EC1118 and S288c taken from NCBI Protein-BLAST results. 37
Figure 16: Superimposition of predicted alcohol O-acetyltransferase (AAT) structures for strain S288c (shown in tan) and strain EC1118 (shown in blue). 38
Figure 17: Superimposition of predicted alcohol O-acetyltransferase (AAT) structures for strain S288c (shown in tan) and strain EC1118 (shown in blue) with #435 mismatched amino acid residue highlighted in green (also marked out by red arrows). 39
Figure 18: Superimposition of predicted alcohol O-acetyltransferase (AAT) structures for strain S288c (shown in tan) and strain EC1118 (shown in blue) with #530 mismatched amino acid residue highlighted in green (also marked out by red arrows). 40
Figure 19: Phylogenetic tree of 45 strains in SGD (SGD, 2014), with strain S288c shown in red, and strain EC1118 underlined in red. 41
Figure 20: NetLogo simulation: wine view fermentation initialization.. 43
Figure 21: NetLogo simulation: wine view fermentation final stage. 44
Figure 22: NetLogo simulation: yeast view fermentation initialization. 46
Figure 23: NetLogo simulation: yeast view mid-progression with normal AAT level. 47
Figure 24: NetLogo simulation: yeast view mid-progression with overexpressed AATs. 48
Figure 25: NetLogo simulation: yeast view mid-progression with Reaction Monitor on.. 49
Figure 26: Bradford Assay Standard Curve 63

LIST OF TABLES

Table 1: Fermentation Flasks Set Up 9
Table 2: Synthetic Wine Must Composition 12
Table 3: Primer Information for ATF2 gene and actin control 18
Table 4: Collective Results of All Bioassays (Tasting Panel Evaluations, RT-PCR, Bradford Assay, and GC-MS) 26
Table 5: Tasting Panel Score Overview 31
Table 6: Calculated Protein Concentration for All Flasks 35
Table 7: Bradford Assay BSA Standard OD Reading 62

ABSTRACT

In order to produce a pleasing aroma in wine, the sugar source provided by the grapes, after going through various biosynthetic pathways catalyzed by various kinds of enzymes in Saccharomyces cerevisiae (wine yeast), forms a variety of aroma-related chemical compounds (Swiegers, Bartowsky, Henschke & Pretorius, 2005). The wet lab section of this project focused on the production of esters in wine through the acetyl-CoA metabolism pathway, catalyzed by alcohol O-acetyletransferase (AAT), which is translated from the ATF2 gene in wine yeast. By monitoring the level of ATF2 gene expression, as well as ester production in the wine fermentation process under various pH values, temperatures, nitrogen levels, and sugar contents, we investigated the fermentation conditions for a desirable ester profile of wine aroma. Although there was no strong evidence of any particular conditions that would boost ester production, the results have given us a few conditions that yields enjoyable aroma profile in wine. In the future, the conditions could be applied to more wine fermentation experiments using grape juice rather than synthetic wine must used in this project, so that the market value of such conditions can be investigated and evaluated.

The modeling section of the project summarized the wine fermentation process from a different perspective. Since the protein folding structure has not been determined experimentally, a protein structure prediction tool MODELLER was used to computationally predict the folded structure of the AAT protein in both strain S288c, the standard lab strain, and strain EC1118, a strain commonly used to produce commercial wine. We also generated a phylogenetic tree based on the multiple sequence alignment results of several yeast strains with regard to the ATF2 gene.

A NetLogo simulation of the wine fermentation process was created to demonstrate the molecular interactions that occur in yeast cells during wine production. The simulation provided a visual aid to students in the field of winemaking while introducing the indispensable role of yeast cells in the wine fermentation process. The simulation also provided control over the temperature of the simulated wine fermentation environment, encouraging the student users to investigate how a change of temperature could influence

the results of pigment extraction and aroma composition in wine. In the future the simulation will be evaluated by the professors at the Wine Research Center of University of Nova Gorica in Slovenia and will be further improved based on the teaching needs of the University.

1. BACKGROUND

Ever since the first winery was discovered in Armenian caves (Owen, 2011), the perfection of wine profile as well as unconventional flavors has been the goal of wine production. By varying the yeast strains, grape strains, pH values, temperatures, nutrient levels, time spans, and even micro-maneuvering the weather conditions, the wine profile can be well-controlled or innovatively altered (Robinson & Harding, 2015). While the taste of wine perceived by the human tongue is limited to sweetness, sourness, bitterness, savoriness, and saltiness (Frank & Hettinger, 2005), a more complete composition of wine aroma is perceived by olfaction and interpreted by the olfactory bulb in human brain (Robinson & Harding, 2015). Therefore, the chemical compounds in wine that contribute to the wine aroma are quintessential to wine production. This project aimed to achieve higher ester level in wine by altering fermentation conditions, as well as contributing the results to the teaching repertoire of the Wine Research Center of University of Nova Gorica at Slovenia.

1.1 Wine Profile

Three major steps comprise the wine tasting process: observing, sniffing/smelling, and tasting/aftertasting (Jackson, 2002). Therefore, the appearance, aroma, and taste of wine comprise the wine profile.

1.2 Wine Aroma

Volatile chemical compounds, such as phenols, esters, alcohols, aldehydes, and acetates, evaporate into air easily, and therefore yield the wine aroma (Rapp & Mandery, 1986). Phenols yield barnyard or medicinal flavor; esters yield fruity, floral, or sweet flavors; alcohols yield spiritous or grassy flavors; aldehydes yield bruised apple flavor; acetates yield fruity or floral flavors (Swiegers, Bartowsky, Henschke & Pretorius, 2005). The compounds either are developed during the fermentation process as byproducts of the transformation of sugar to alcohol, or further being developed after being bottled and stored (Swiegers, Bartowsky, Henschke & Pretorius, 2005). Due to the time limitation, the project only considered the compounds developed during and right after the fermentation process.

1.3 Biosynthetic Pathways in Yeast Fermentation

Wine fermentation was one of the earliest food production processes discovered and developed by human (Dashko, et al., 2014). The use of yeast has also been well studied over the years. It has been discovered that the wine fermenting yeast strain *Saccharomyces cerevisiae* is positive for Crabtree effect. Crabtree effect is a phenomenon that describes the *S. cerevisiae* being able to switch on the fermentation mode aerobically when sugar level in the environment is high (Crabtree, 1928). The specific sugar concentration threshold where the Crabtree effect can be observed varies for different Crabtree effect positive yeast strains (Dashko, et al., 2014). The threshold is 0.2% glucose for *S. cerevisiae* (Postma, et al., 1989).

Since yeast is one of the most well studied biological models, the biosynthetic pathways catalyzed by yeast enzymes during fermentation have been identified (Figure 1).

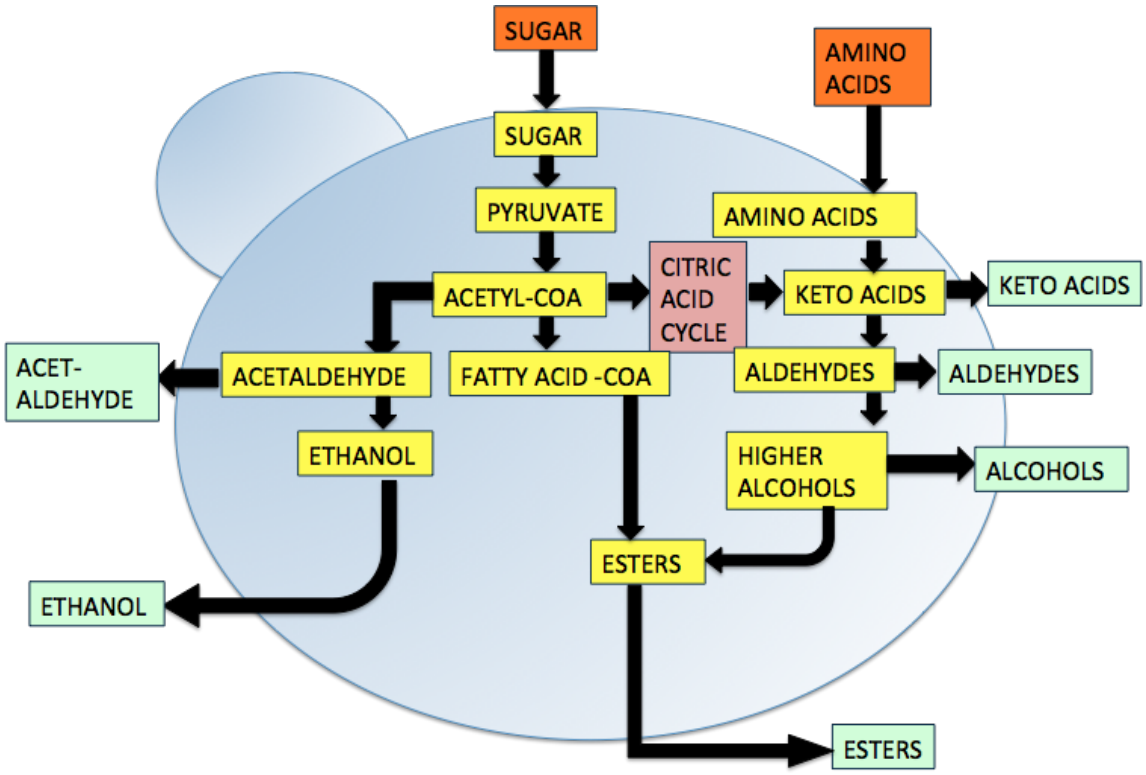

Figure 1: Major Biochemical Pathways in Yeast Fermentation (Adapted from Biochemistry, Voet & Voet, 2013)

It can be seen in Figure 1 that the yeast cells conduct a variety of biochemical reactions during wine fermentation. The major energy inputs are sugar and amino acids, and the major outputs are ethanol and a combination of aroma-related compounds.

1.3.1 Ethanol Production Pathway

Ethanol is one of the major products of yeast fermentation pathways (Figure 1). The first step to ethanol production is glycolysis (Voet, Voet, & Pratt, 2013). The reaction can be seen below:

$$\text{Glucose} + 2\ NAD^+ + 2\ ADP + Pi \rightarrow 2\ \text{Pyruvate} + 2\ NADH + 2\ ATP + 2\ H_2O + 2\ H^+$$

The second step is alcoholic fermentation (Voet, Voet, & Pratt, 2013). The reaction can be seen below:

$$\text{Pyruvate} \xrightarrow{\text{Pyruvate decarboxylase}} \text{Acetaldehyde}$$

$$\text{Acetaldehyde} + NAD^+ \xrightarrow{\text{Alcohol dehydrogenase}} NADH + \text{Ethanol}$$

Specifically, the enzyme that catalyzes the reaction of acetaldehyde-to-ethanol is Yeast Alcohol Dehydrogenase (YADH).

1.3.2 Ester Production Pathway

The ester production pathway is similar to the ethanol production pathway in the beginning but later diverges (Pires, et al., 2014). The first step is glycolysis:

$$\text{Glucose} + 2\ NAD^+ + 2\ ADP + Pi \rightarrow 2\ \text{Pyruvate} + 2\ NADH + 2\ ATP + 2\ H_2O + 2\ H^+$$

The second step is the initiation of the Citric Cycle:

$$\text{Pyruvate} + CoASH + NAD^+ \xrightarrow{\text{Pyruvate dehydrogenase}} CO_2 + NADH + \text{Acetyl-CoA}$$

Thirdly, higher alcohols in yeast go through esterification reaction with the presence of acetyl-CoA and the assistance of alcohol acetyltransferase (AAT).

$$\text{Acetyl-CoA + Ethanol} \xrightarrow{\text{Alcohol acetyltransferase}} \text{Ethyl acetate}$$

$$\text{Acetyl-CoA + Isoamyl alcohol} \xrightarrow{\text{Alcohol acetyltransferase}} \text{Isoamyl acetate}$$

$$\text{Acetyl-CoA + 2-phenylethanol} \xrightarrow{\text{Alcohol acetyltransferase}} \text{Phenylethyl acetate}$$

Among all aroma-related compounds, this project focused on the production of esters. On the one hand, esters are a group of sugar fermentation end product as seen in Figure 1. They will not further participate in other biological pathways so that the amount of esters produced by fermentation can be measured more accurately than intermediate chemical compounds. On the other hand, esters generally give a pleasant fruity flavor and the project results could potentially give suggestions to the development of novel wine profiles in the future.

Furthermore, the production of ester is catalyzed by the alcohol acetyltransferase (AAT) in yeast, which is translated from the ATF2 gene of yeast (Rapp & Mandery, 1986). Therefore, the living state of yeast cells, the activity of the AAT enzyme, and the expression level of the ATF2 gene can all influence the final ester production level.

1.4 Wine Must

Wine must, also known as “young wine”, is the starting mixture of wine fermentation (Robinson & Harding, 2015). The wine production process utilizes a mixture of crushed grape fruit, skin, and juice, as natural grape must. The must provides various types of sugar, which feeds the yeast cells as well as acting as the substrate of various biochemical pathways. It also provides amino acids, which supports the gene expression within the yeast cells, as well as acting as the substrate of biochemical synthesis of phenolic compounds. In lab research, synthetic grape must is occasionally used. The content of synthetic grape must mimics the contents of the natural grape must to provide the sugar

and essential amino acids so that the fermentation process can progress as it does in natural wine production (Viana, Loureiro-Dias, & Prista, 2014). In addition, because the content of the synthetic wine must is carefully calculated and additional precursors can be added to induce the progression of certain biochemical pathways, the yeast fermentation with synthetic grape must is highly controlled and the results are more predictable than the fermentation with natural grape must. However, the resulting wine product is not for drinking since all components of the wine are lab chemicals and have potential safety concerns.

1.5 The Influence of Environmental Condition Change to Wine Fermentation

The growth and activity of yeast cells in wine must, can be altered by environmental condition changes.

1.5.1 The Influence of pH Value to Wine Fermentation

The acidity of the environment of wine fermentation can affect the stability of the proteins provided by the grape must, the color of the wine, and the flavor of the wine (Kodur, 2011). The production of esters is influenced by the acidity of the fermentation environment as well. Since the esterification reaction is the reaction between acid and alcohol, the more acidic the environment is, the more esters would potentially be produced due to the esterification process being pushed to the product side. It is hypothesized that within the threshold of possible acidity provided by wine must, the lower the pH level is in the fermentation environment, the higher level of esters will be produced as part of the fermentation product.

1.5.2 The Influence of Temperature to Wine Fermentation

Temperature of the environment influences the speed of fermentation. Within the temperature range that the yeast stays viable, the yeast activity is slow under low temperature; the activity increases as the temperature increases; the activity slows down again if the temperature goes too high that the yeast cells start to die. Hence the fermentation process will be the slowest under low temperature, medium length under moderate temperature for the yeast strain, and the fastest under a warm temperature for the yeast strain. The yeast strain used for the project is the industrial level *S. cerevisiae* Lalvin T73 strain. Twenty-two degrees Celsius (22 °C) is the temperature best for yeast

growth of this strain (Rotter, 2008), as well as a working temperature for wine fermentation.

Temperature control also has other influences on wine fermentation. Higher temperatures tend to lead to the loss of alcohol and aroma related chemical compounds through evaporation, since aroma compounds are usually volatile and the fermentation flasks are open to the environment to allow oxygen/carbon dioxide exchange with the environment. Lower temperatures tend to lead to color change and high production of ethyl acetate (Plumpton College, 2015), due to the continuous esterification of alcohol during the prolonged fermentation process. Counting all factors, it is hypothesized that a lower fermentation temperature of 15°C will yield higher ester production, and a higher fermentation temperature of 35°C will yield lower ester production.

1.5.3 The Influence of Glucose/Fructose Ratio on Wine Fermentation

Two major sugar source provided by the grape must are glucose and fructose. Although they are not differentiated in the biochemical pathway of yeast fermentation and will have the same end products chemically, yeast has a slight preference towards glucose comparing to fructose (Tronchoni, Gamero, Arroyo-Lopez, Barrio, & Querol, 2009). It would take longer for yeast to consume the fructose, and fructose will be metabolized only when the glucose in the environment is exhausted and a higher level of ethanol is present in the fermentation environment. Therefore it is hypothesized that the amount of esters produced from the sugar source will be approximately the same for different glucose/fructose composition. Moreover, the fermentation flask containing more fructose will take longer time to complete the process, and the extended time will give the higher alcohol in the environment more time to be further processed into esters. It is hypothesized that the fermentation flask containing more fructose than glucose could potentially yield higher level of esters.

1.5.4 The Influence of Nitrogen Level to Wine Fermentation

Nitrogen source provides the precursors for protein synthesis within the yeast cells, hence its important role in the growth and activity of yeast in the fermentation process. Nitrogen deprivation could induce a delay or even a complete halt to the fermentation process and ammonium salts are added to the grape must to prevent nitrogen starvation in wine

industry. (Jimenez-Marti, Aranda, Mendes-Ferreira, Mendes-Faia, & li del Olmo, 2007) This project uses ammonia sulfate as the source of nitrogen in the fermentation environment. It is hypothesized that the ester production will increase as the nitrogen level in the fermentation environment increases, since the yeast growth and catabolism activities increases under higher level of nitrogen.

In summary, it was predicted that the ester component of the wine aroma would change under the change of fermentation conditions: pH level, temperature, glucose/fructose ratio, and nitrogen level. Lower pH level, higher temperature, higher fructose concentration, and higher nitrogen level were predicted to be more optimum conditions for higher ester production.

1.6 Bioinformatics in Wine Research

The function of the ATF2 gene as well as the AAT enzyme is well known in the wine research field however the structure of the AAT enzyme has not been determined experimentally. We predicted the structure of the alcohol O-acetyltransferase using a strong structural modeling tool MODELLER (Fiser & Sali, 2003), and compared the predicted structure of the AAT enzyme between two yeast strains. One strain selected was the S288c strain used in the project wine fermentation; the other strain selected was the EC1118 used in commercial wine production. Superimposition of the two predicted protein structures provided insight on the variances between the same enzymes in different yeast strains. It was hypothesized that the structure of the AAT enzyme between the two strains would be mostly superimposable but slightly different, suggesting a structural reasoning behind the various ester profiles in wine. Furthermore, the genetic distance between the two strains with regard to the ATF2 gene was visualized through a phylogenetic tree. It was hypothesized that the distance between the two strains should be very small since they are two strains of the same species, *Saccharomyces cerevisiae*.

1.7 Virtual Wine Fermentation Simulation

Visual simulation of biological processes can provide effective visualization of complex biological systems and can be used to test scientific hypothesis (Wilensky, 2016). To

provide visual aids to wine school students at the University of Nova Gorica at Slovenia, a simulation of the wine fermentation process, both in the view of the fermentation flasks and in the view of individual yeast cells, was designed using a modeling language NetLogo. NetLogo has strong features to support visualization designs and also provides a rich library of modeling examples. The language also provides user interfaces, allowing end users to control the start/stop of the simulation, as well as adjust certain parameters of the simulation to interactively learn the effect of such parameters. It was hypothesized that by simulating the wine fermentation process according to the biochemical pathway of alcohol fermentation mediated by yeast cells, the final amount of ethanol and esters being produced would be close to the common ethanol and ester level for commercial red wine.

2. MATERIALS AND METHODS

2.1 Fermentation Set Up

According to the hypothesis proposed and the experimental design, 18 wide mouthed 250 mL shake flasks were set up for various conditions of wine fermentation. The recipe and other recommendations for the fermentation were provided by the Wine Research Center at University of Nova Gorica in Slovenia. Table 1 below shows the flasks numbers and the fermentation conditions they correspond to.

Table 1: Fermentation Flasks Set Up

Flask No.	Condition	pH	Temperature/°C	Sugar Content (Glucose: Fructose)	Nitrogen Content
1	Control	3.4	22	1:1	0.6g/L
2	Low pH	3.0	22	1:1	0.6g/L
3	High pH	4.0	22	1:1	0.6g/L
4	Low Temperature	3.4	15	1:1	0.6g/L
5	High Temperature	3.4	35	1:1	0.6g/L
6	Low Glucose, High Fructose	3.4	22	1:2	0.6g/L
7	High Glucose, Low Fructose	3.4	22	2:1	0.6g/L
8	Low Nitrogen	3.4	22	1:1	0.1g/L
9	High Nitrogen	3.4	22	1:1	5g/L

Flask 10 was made under the control conditions and was used as sugar level monitor group. The experiment was performed twice (n=2) for each experimental and control condition.

2.1.1 Inoculum

The yeast strain used for the wine fermentation was the *Saccharomyces cerevisiae* T73 Lalvin provided by the Wine Research Center of University of Nova Gorica in Slovenia. The yeast strain preserved in - 80°C was first thawed and plated aseptically on a yeast peptone dextrose (YPD) plate and left on the benchtop under room temperature to grow for 120 hours. A duplicate plate was streaked as well to ensure yeast colony growth.

One (1) liter of yeast peptone dextrose solution was prepared with 1% yeast extract (Biolife), 1% peptone (Biolife), and 2% dextrose (Sigma-Aldrich) and the pH value of the solution was adjusted with either 10 M HCl solution or 10 M NaOH solution to 6.2. The solution was then autoclaved to ensure sterility.

After 120 hours of growth on the YPD plate, 3 colonies with a diameter of 3 mm were carefully picked with a clean toothpick and aseptically transferred to 3 mL of autoclaved YPD solution in a clean test tube. The plates were sampled 5 times in total, and the test tubes were incubated with 100 rpm agitation in a 25°C incubator for 24 hours.

After 24 hours of incubation, the cell number inside of the test tubes was estimated using spectrophotometer. The spectrophotometer was set to optical density (OD) 600 and water was used as the blank sample. A 1:8 dilution of the well-mixed test tube content had an OD600 of 0.963. It was estimated that 0.13 mL of the well-mixed test tube content contained 1 OD unit of yeast cells.

Then 1.5 mL of the well-mixed test tube content was added aseptically to a shake flask containing 50 mL of sterile YPD solution. Three (3) of these flasks were prepared to ensure sterility and they were capped with paper stoppers. The flasks were incubated with 200 rpm agitation in a 25°C incubator for 24 hours.

After 24 hours the number of yeast cells in the flasks was estimated again using a spectrophotometer. The flasks had an OD600 of approximately 11 OD units per milliliter. Twenty (20) OD units of cells were needed for a 250 mL fermentation flask inoculation. Hence 1.82 mL of inoculum flask content contained the amount of cells needed for the inoculation of each flask.

Following the calculation, 1.82 mL of inoculum flask content was aseptically added to a sterile 2mL Eppendorf tube. Eighteen (18) Eppendorf tubes were prepared for 18 sets of fermentation flasks following the experimental design. The Eppendorf tubes were then centrifuged at 3000 x g for 5 minutes. The supernatant YPD solution was carefully removed and the yeast cells were washed and resuspended in 10% glucose solution. The cells were centrifuged again at 3000 x g for 5 minutes. The glucose solution was used again to resuspend the cells. The yeast cells were left in the glucose solution under room temperature to adjust to a high glucose environment.

2.1.2 Synthetic Wine Must

The contents of the synthetic wine must resemble the contents of the natural wine must. The synthetic wine must components used for the fermentation flasks are listed in Table 2.

Table 2: Synthetic Wine Must Composition

Content	**Amount (g/L)**	**Vendor**
L-Alanine	0.1	AppliChem
L-Arginine	0.302	Sigma
L-Aspartic Acid	0.05	AppliChem
L-Cysteine	0.005	AppliChem
L-Glutamic Acid	0.075	Sigma
L-Glutamine	0.125	Sigma
L-Glycine	0.05	Sigma
L-Histidine	0.02	Sigma-Aldrich
L-Isoleucine	0.025	AppliChem
L-Leucine	0.025	Sigma
L-Lysine	0.006	Sigma
L-Methionine	0.01	Sigma-Aldrich
L-Phenylalanine	0.0375	Sigma
L-Proline	0.075	AppliChem
L-Serine	0.05	Sigma
L-Threonine	0.075	Sigma-Aldrich
L-Tryptophan	0.01	Sigma-Aldrich
L-Tyrosine	0.01	Sigma
L-Valine	0.025	Sigma-Aldrich
Ammonia Sulfate	0.612	Emsure
Citric Acid	0.2	Sigma

L-Tartaric Acid	3	Emsure
L-Malic Acid	2	Sigma
Yeast Nitrogen Base	6.65	Fluka
D-Glucose	120 for 1:1 conditions, 80 for low glucose condition, and 160 for high glucose condition	Sigma-Aldrich
D-Fructose	120 for 1:1 conditions, 80 for low fructose condition, and 160 for high fructose condition	Carl Roth

The must was prepared first with all the corresponding components. Then the pH of the must was adjusted with HCl or NaOH solution (10 M) to required experimental condition. Finally, the must was vacuum filtered with 500 mL Millipore 0.22 µm sterile filter unit and aseptically added to each flask.

2.1.3 Inoculation and Fermentation

The flasks were then inoculated with the yeast cells in glucose solution. One (1) Eppendorf tube of cells was added to one flask in the laminar flow hood. The flasks were then capped with airlock stopper wiped with 50% ethanol, dried in the hood, and sealed with water. Finally, the capped flasks were put into respective incubators with preset temperatures and zero agitation. The final flask set up can be seen in Figure 2 below.

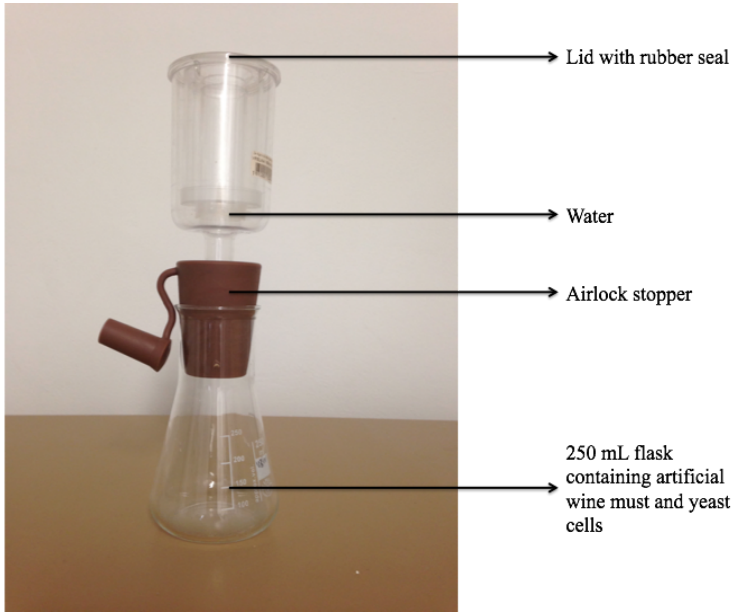

Figure 2: Fermentation Flask Final Set Up

The water seal also indicated the progress of the fermentation process. The top lid floated in the water after set up. As the fermentation process went on, the oxygen inside of the flasks was gradually consumed and the lower pressure in the flask pulled the floating lid downwards.

The high temperature and low temperature incubators can be seen in Figure 3 and Figure 4 below. The room temperature flasks were placed in the shaded area of an air-conditioned room with the temperature set to 22°C.

Figure 3: Incubator Set at 35°C

Figure 4: Incubator Set at 15°C

2.2 Sugar Content Monitoring

The sugar level of the flask content was monitored twice a week through flask 20 using a refractometer. The refractometer is commonly used in the food industry to measure the level of sugar in a mixture. The data read from the refractometer is in the unit of degree Oechsle (°Oe). One (1) °Oe measures 1 gram of weight difference between 1 liter sample wine must and 1 kg (weight of 1 liter water) (Wines of Germany, 2003). The precision of the refractometer varies depending on the mixture composition, but in general it gives a close estimate of the wine fermentation mixture in this project. The fermentation process was seen as terminated when the refractometer reading of the fermentation flasks approached 10 °Oe.

At the end of fermentation process of each flask, samples were collected for analysis of ATF2 gene expression, and for evaluation of ester production levels.

2.3 Ester Level Detection and Measurement

The ester level of the wine product at the end of fermentation process was first examined from the supernatant of the flask contents.

2.3.1 Wine Preservation

To preserve the ester as well as other volatile chemical compounds in the final wine product, the wine sample was taken and preserved with anti-fermentation solution. The anti-fermentation solution contains 1g of sodium azide (Sigma-Aldrich) and 0.01g of L-ascorbic acid (Sigma-Aldrich) in 1 liter of molecular quality water. The wine product sample was preserved by adding 1 mL of anti-fermentation solution into 9 mL of sample in a sterile 15mL conical tube, and the samples were stored at -20°C.

2.3.2 Gas Chromatography – Mass Spectrometry

Gas Chromatography – Mass Spectrometry (GC-MS) is an analytical method that combines the substance chromatography by boiling point and a mass spectrum to identify different substances in an unknown mixture (Grob, 2004). The method was performed in the chemistry analytical lab at Worcester Polytechnic Institute, instructed by Professor Drew Brodeur. One (1) mL liquid of each sample (Sample 1-9) was bottled for the GC-MS instrument and the standard analytical procedure was run for each sample.

2.3.3 Wine Tasting Panel

The wine samples were stored in 125 mL brown glass bottle with plastic seal screw cap at 4°C. Marbles were added to the bottles after the bottles were filled with wine to ensure least aeration to the wine. Since a lot of the wine aroma compounds are volatile, contact between wine and air would allow the aroma compounds to escape into the air. The lost of aromatic compounds would further compromise the wine tasting results, so the less aeration was given to the wine, the better.

A group of professional wine degustators was invited to evaluate the wine samples. They evaluated the wine aroma with a focus on ester compositions. The common ester related flavors being evaluated were: citrus fruit, apple/pear, banana, berries, flowery flavor, spices, and honey. The wine tasting evaluation sheet can be seen in Appendix A.

2.4 RNA Extraction

To evaluate the ATF2 gene expression at the transcriptional level, the total RNA was extracted from each sample. To comply with the RNA Extraction Kit (QIAGEN) capacity, 1.6 OD units of yeast cells was taken from each flask, added into an Eppendorf tube, and centrifuged at 1,000 x g for 1 minute. The supernatant was removed and the cells were resuspended and washed with molecular quality water and centrifuged again. The cells were resuspended in 600 µL QIAzol Lysis Reagent (QIAGEN). Three hundred (300) microliters of 0.5mm glass beads were added to each tube and the tubes were vortexed for 5 minutes. The glass beads were then allowed to settle and the supernatant was transferred to new Eppendorf tubes and centrifuged at 16,000 x g for 2 minutes. The supernatant was again transferred to new centrifuge tubes and rested on benchtop for 5 minutes. The RNeasy Mini Kit (QIAGEN) was used to extract RNA from the thawed samples according to the manufacturer's protocol. The final eluted RNAs were stored at -80°C until samples from all flasks were processed.

2.5 RT-PCR and Agarose Gel Electrophoresis

The RNA was reverse transcribed into complementary DNA (cDNA) first for stabilization and preparation for the polymerase chain reaction (PCR). For each sample taken from the fermentation flasks, 32 ng RNA extract and 4 µL of Quanta Biosciences qScript reagents (containing optimized concentrations of $MgCl_2$, dNTPs, recombinant RNase inhibitor protein, qScript reverse transcriptase, random primers, oligo(dT) primer, and stabilizers) were well mixed in an Eppendorf tube and incubated at 25°C for 5 minutes, 42°C for 30 minutes, 85°C for 5 minutes, and held at 4°C.

Then 3 µL of the reverse transcribed cDNA for each flask was taken out and added to a new 0.2 mL microtube along with 1.5 µL of 10 µM upstream primer, 1.5 µL of 10µM downstream primer, 6.5 µL of nuclease free water, and 12.5 µL of GoTaq Master Green Mix (Promega). The PCR cycler was pre-programmed and pre-heated and the mixture was incubated at 95°C for 2 minutes; then at 95°C for 45 seconds, 57°C (annealing temperature of designed primers) for 45 seconds, and 72°C for 15 seconds for 30 cycles in total; at last the tubes were incubated at 72°C for 5 minutes and held at 4°C.

The actin control of each sample was made in 0.2 mL microtube by mixing 3 µL of cDNA, 3 µL of 10µM actin forward and reverse primer, 6.5 µL of nuclease free water, and 12.5 µL of GoTaq Master Green Mix (Promega). The actin controls were amplified along with the ATF2 gene primer samples.

The primer information for the ATF2 gene and the actin control can be seen in Table 3 below.

Table 3: Primer Information for ATF2 gene and actin control

Gene	NCBI Gene ID	Upstream Primer Sequence (5' - 3')	Downstream Primer Sequence (5' - 3')	Amplicon Length (bp)	Vendor
ATF2	853088	GCAGAACGAT TCCCATTCGC	AGTGGTCACC GTTGTCGTAC	322	Integrated DNA Technologies
Actin	60	AGAGCTACGA GCTGCCTGAC	GGATGCCACA GGACTCCA	184	Integrated DNA Technologies

The agarose gel was pre-made for the gel electrophoresis. The percentage of the gel was 2%, for DNA products of 50 - 2000 base pairs (Promega Corporation, 2015). One (1) gram of agarose (Sigma) and 50 mL 1X Tris-Acetate-EDTA (TAE, consists of 40mM Tris, 20mM acetic acid, and 1mM EDTA) was well mixed and microwaved until the mixture was completely melted. Five (5) µL ethidium bromide (AppliChem) was then carefully added to the mixture and well mixed. The mixture was then poured into the electrophoresis chamber with a comb inserted close to one end of the chamber, and was left in the chamber to harden. The running buffer of the electrophoresis also consists of 1X TAE and 5µL of ethidium bromide (AppliChem).

The ladder for the electrophoresis was made in 0.2 mL microtube by mixing 6 µL of DNA 100 bp Low Ladder (Sigma), 6.5 µL of nuclease free water (QIAGEN), and 12.5 µL of GoTaq Master Green Mix (Promega). One ladder mix was made for each gel.

Ten (10) µL of the PCR product was carefully pipetted into the well formed around the comb teeth, one sample per well. Each gel contained 1 ladder, 3 ATF2 gene primer samples, and 3 actin controls. Then the chamber was connected with the power source and PCR products were separated for 40 minutes at 80 Volts each for the final results.

2.6 Bradford Assay

To evaluate the gene expression on the translational level, a Bradford Assay was performed to determine the total amount of protein translated in 5 OD units of yeast cells.

Five (5) OD units of yeast cells were first centrifuged down at 1,000 x g for 3 minutes. The supernatant was discarded. The cells were resuspended in water and centrifuged down again. The cells were lysed and homogenized following the start of the RNA extraction procedure recommended by the QIAGEN RNeasy Mini Kit manual. The cells were resuspended in 600 µL QIAzol Lysis Reagent (QIAGEN). Three hundred (300) microliters of 0.5mm glass beads were added to each tube and the tubes were vortexed for 5 minutes. The glass beads were then allowed to settle and the supernatant was transferred to new Eppendorf tubes and centrifuged at 16,000 x g for 2 minutes. The supernatant was again transferred to new centrifuge tubes and rested on benchtop for 5 minutes. Then 180 µL of chloroform (Sigma) was added to each tube and the mixture was vigorously shaken for 15 seconds. The tubes were then centrifuged for 15 minutes at 12,000 x g, 4°C. The supernatant was transferred to a new Eppendorf tube after the centrifugation.

After lysing the yeast cells with glass beads, 20 µL of the cell lysate was added to a new Eppendorf tube containing 1 mL Bradford Reagent (Sigma-Aldrich). The same was done for all samples, and the Eppendorf tubes were set on benchtop for 5 minutes so that the dye and the protein can bind with each other. The OD595 value of the samples was read in the spectrophotometer.

The standard for Bradford Assay was established with a serial dilution of bovine serum albumin (BSA, ChemCruz).

2.7 Bioinformatics

2.7.1 Protein Sequence Alignment

The complete protein sequence of AAT encoded by the ATF2 gene of strain S288c and strain EC1118 was downloaded in FASTA format from Saccharomyces Genome Database (SGD, 2016). NCBI Protein-BLAST was then used to compare the two protein sequences (Altschul et al, 1990).

2.7.2 Structure Prediction and Comparison

At the beginning of the research a search of the existing protein structure was done on PDB in hopes of getting experimental protein structures so that UCSF Chimera could be directly applied on the structural information to conduct a structural comparison. However, no valuable results returned for the target protein. Therefore, MODELLER was used in this project to provide computational protein structures of the ATF2 gene.

To establish a computational structure, the target protein sequence needs to be aligned with a template sequence. The ATF2 protein sequence of strain EC1118 and strain S288c were obtained from the Saccharomyces Genome Database (SGD, 2016). Protein Model Portal (PMP, 2016) was used to search for the template sequence. PMP partners with several protein modeling databases and provides a single interface to query its partner databases simultaneously. The structural information of the best-fitted template was then downloaded from Protein Data Bank (PDB, 2016). To establish a structural model prediction for the target protein sequence, MODELLER took in the target sequence and the structure of the modeling template, and 5 predictions were calculated for the target sequence of each strain.

To evaluate the protein structure prediction results, all five models of the same strain were imported into UCSF Chimera and superimposed (Huang et al, 1996). If all five structures were similar to each other, then the prediction was considered successful. Discrete Optimized Protein Energy (DOPE) is a statistical value used by MODELLER to assess its model predictions (Fiser & Sali, 2003). The structure with the lowest DOPE was considered the best structural prediction for each sequence to conduct final

superimposition and comparison. Finally, the best predicted structure for each strain was imported into UCSF Chimera and the MatchMaker tool was used to superimpose the two structures.

2.7.3 Phylogenetic Tree

SGD generates a phylogenetic tree for all 45 strains the database contains genetic information on, with regard to the gene of interest. To produce the tree visualization, SGD first generated a multiple sequence alignment from the protein sequence of the AAT enzyme in several yeast strains, and then generated the phylogenetic tree using ClustalW (SGD, 2016).

2.8 Wine: Simulation Overview, Design Concepts, and Details (ODD)

The simulation was coded using NetLogo written by Uri Wilensky (Wilensky, 2016). The design of the simulation was based on the data collected in the biological section of this project and past research regarding wine fermentation. Here, the standard ODD is used to describe the model (Railsback & Grimm, 2012).

2.8.1 Purpose

The model was designed to demonstrate the major biochemical pathways in wine fermentation and explore questions about ethanol percentage and ester profile formation in wine. Does the experimentally determined ethanol percentage and ester amount in wine make sense if all molecules interact according to the chemical formula? How does the soaking temperature affect the color of the wine? How does the fermenting temperature affect the production of ethanol and esters? How does overexpressing certain gene(s) influence the production of related chemicals?

2.8.2 Entities, State Variables, and Scales

The model has two parts of visualization: wine view and yeast view.

The wine view contains yeast cells, glucose (one mmole per agent), ethanol (one mmole per agent), and ester (one mmole per agent). The patches make up a square grid wine fermentation solution of 32 x 32 patches. The color of the patches represents the color of the wine. The yeast cells are created in patches with a y-coordinate lower than -10, representing the yeasts' stationary presence at the bottom of the fermentation apparatus.

The glucose, ethanol, and ester agents are created at random coordinates and float around in a random movement pattern. The collision between the agents represents the chemical reactions. All chemical molecules are of the same size, but the yeast cells are 6 times larger than the molecules to show that the sizes of chemical molecules and biological cells are very different in scale.

The yeast view contains glucose, pyruvate, ethanol, ester, sugar transporters, glycolysis enzyme complex, pyruvate decarboxylase, and the AAT protein. The patches make up a square grid of 32 x 32 patches. The color of the patches with an x-coordinate higher than or equal to 11 represents the color of the wine, and the rest of the patches are set to color grey, representing the inside of a yeast cell. The glucose agents are created at random coordinates outside of the yeast cell region and the yeast enzymes are created at random coordinates inside of the yeast cell region. At the borderline between the two regions, sugar transporters are created. The glucose molecules can only enter the yeast cell region upon collision with the sugar transporters, and they are much smaller molecules compared with the transporters and the enzymes. Again the size disparity is only to conceptually show the users the scale difference between chemical molecules and biological macromolecules, and does not reflect any real sizes.

2.8.3 Process Overview and Scheduling

Both the wine view and the yeast view have the "Cold Soak" process. The crushed grape fruit and juice need to be collected and placed under low temperature so that the coloring molecules of the fruit can go into the liquid and the wine product can be colored properly. This process will advance the color of the patches over time and the final patch color is determined by the user selection of the soaking temperature.

There are 3 processes in the wine view: the molecules' creation and movement, the yeast cells growing, and the collision between the molecules and the yeast cells. Only glucose molecules and yeast cells are created after setting up the fermentation environment. The yeast cells remain stationary and the glucose molecules diffuse in the environment. Upon collision of a glucose agent and the yeast cell agent, the glucose disappears and creates one ester agent in a 1/90 chance, while other times the collision creates one ethanol agent.

This process stops when there are only 10 glucose agents left, which approximates a concentration of 7.2g/L, a typical point where a red wine fermentation is halted. The number of yeast cells increments 1 in a 1/10 chance after each tick to simulate a 0.1OD/hour yeast growth rate, and stops at 500. In this view of the simulation one tick corresponds to one hour in real time.

There are 2 processes in the yeast view: the molecules' creation and movement, and the collision between the molecules and the proteins (transporters and enzymes). The set up of the environments separate the canvas into two areas: the wine liquid environment (color of the wine after cold soaking), and inside of the yeast (grey). The border between the two areas is guarded by sugar transporters. The glucose molecules were created outside of the yeast and move once in a random direction per time step, and can only enter the yeast if they collide with a sugar transporter. The glycolysis enzyme complex (green), pyruvate decarboxylase (orange) and alcohol O-acetyltransferase (blue), were created inside of the yeast cell, and can move in a random direction once per time step but cannot leave the cell. Each glucose molecule agent, when colliding with a glycolysis enzyme complex, hatches 2 pyruvates, and then dies. The pyruvates then collide with either pyruvate decarboxylases (PDCs) or alcohol O-acetyltransferases (AATs). The collision with PDCs will create one ethanol molecule and kill the pyruvate; the collision with AATs will create one ester molecule in a 1/10 chance to make up for the PDC and AAT abundance disparity in the yeast cells, also kills the pyruvate. The created molecules, ethanol and esters, were diffused out of the yeast cell region. Since the ethanol and ester concentration will always be higher inside of the yeast cell than outside in the wine, the diffusion movement set the ethanol and ester molecules to move heading towards the outside of the yeast cell.

There are two extra switches in the yeast view that slightly alters the processes described above. When the "Overexpression" switch is on, 10 times more AATs are created at the environment set up, which simulates an overexpression of the ATF2 gene, which translates to higher abundance of AATs. When the "Reaction Monitor" switch is on, the glucose molecules does not die after colliding with the glycolysis enzyme complex.

Instead they turn into dark brown color so that the users are able to see the before/after-collision effects. The dark brown glucose agent can no longer interact with other molecules in the environment.

2.8.4 Design Concepts

The simulation is built on the theoretical biochemical pathways of ethanol and ester production happening in wine fermentation with the assistance of yeast cells. These two pathways are addressed in the yeast view by showing the users the exact molecular interactions according to the chemical equations. The movement of the molecules resembles what really happens in and out of a cell. On the other hand, the two pathways are addressed in the wine view by simulating the interactions in the unit of moles. The simulation converts the amount in moles into the amount in the convenient measuring unit for each type of chemicals respectively. For instance, the amount of glucose molecules in the wine environment is presented as g/L, and the amount of ethanol in the wine is presented as volume percentage.

Sensing in this simulation is addressed by the molecules movement pattern change based on the environmental temperature change. As the fermentation temperature increases, the agents move faster, and presumably collide more often with other agents.

The *interactions* among the agents play a key role in this model. Each collision of the enzyme and its corresponding substrate simulates a chemical reaction and the correct actions of each agent after the collision is key to the outcome of this simulation.

Stochasticity is used to represent some sources of variability in both views that are too complex to represent mechanistically. In the wine view, the movement of all chemical molecules are random, and the creation of yeast cells is at random positions and a 1:10 chance. The creation of ethanol and ester molecules is in a chance of 89:90 and 1:90, respectively. In the yeast view, the amount of AATs is set to only be 10 times less than the amount of PDCs and glycolysis enzyme complexes. In reality this abundance disparity is 1:90, however a realistic simulation would make the AATs really difficult to see and the space really easily over crowded by agents. Therefore, the program only

shows a 1:10 difference in the amounts of enzymes, but set the esters to be produced in a 1/9 chance upon each collision. This way the 1:90 enzyme abundance disparity is maintained, and the visualization is clearer to the users as well.

The two views are *observed* through different channels. The wine view output is observed through the monitors. Each monitor counts the existing number of each agent in the view and does calculations to convert the number of agents (also number of moles) into common measure units of each molecule. The output of the yeast view, on the other hand, is observed through the monitors as well as a plot. The monitors show the numbers of agents existing in the view respectively. The plot not only shows the number of agents in the view, but also shows the speed of each molecule's production over time.

2.8.5 Initialization

The view is initialized as a black background. The background color is determined by the cold soak process. The fermentation process of wine view is initialized by having the initial amount of yeast cells at the bottom of the view and the initial amount of glucose molecules scattered in the view. The fermentation process of yeast view is initialized by having the yeast cell region colored grey, the sugar transporters located at the border of the cell membrane, the glucose molecules scattered outside of the cell region, and the enzymes scattered inside of the cell region.

3. RESULTS

To investigate whether different wine fermentation conditions are able to produce notable ester aroma profile in wine, we varied the pH value, glucose/fructose ratio, and nitrogen level in the artificial wine must and the fermentation temperature. We then fermented the artificial must per wine fermentation procedure using the lab yeast strain S288c. After the fermentation process, we evaluated the AAT enzyme RNA transcription level, the overall protein translation level, and the resulting ester production level. We would like to investigate whether certain wine fermentation conditions would increase the AAT enzyme level in yeast, and whether the increased level of such enzyme would increase the esters in wine aroma. A collective result of all assays can be seen in Table 4 below.

Table 4: Collective Results of All Bioassays (Tasting Panel Evaluations, RT-PCR, Bradford Assay, and GC-MS)

Sample Number	**1**	**2**	**3**	**4**	**5**	**6**	**7**	**8**	**9**
Fermentation Conditions	Control: pH 3.4, 22 °C, G:F = 1:1, N: 0.6g/L	Low pH: 3.0	High pH: 4.0	Low Temp: 15 °C	High Temp: 35 °C	G:F = 1:2	G:F = 2:1	N: 0.1g/L	N: 5g/L
Tasting Panel	N/A	4	0	3	3	1	1	1	4
RT-PCR	☒	✓	✓	☒	☒	☒	✓✓	☒	✓✓✓
Bradford Assay	N/A	🡻🡻	🡻🡻	🡻	🡹	🡻	🡹🡹	🡻	🡻
GC-MS	No notable results overall. Sample 8 reported presence of phenylethyl alcohol, which has a pleasant floral odor.								

Legend:
Tasting Panel Results:
number represents the number of ester aroma features that were scored at least by one panel judge that was better than the sample fermented by the standard control conditions;
RT-PCR Results:
cross represents no visible signal on the electrophoresis gel;
check mark represents visible signal on the gel, and number of check marks represents the strength of signal on the gel;

Bradford Assay Results: the arrow represents spectrophotometer readings lower (down arrow) or higher (up arrow) than the sample fermented by the standard control conditions, the number of arrows represents the level of difference.

The detailed results of all assays are shown in section 3.1 through section 3.5 below.

To develop an educational tool for the students in Wine Research Center of University of Nova Gorica at Slovenia to understand the molecular interactions happening inside of the yeast cells during wine fermentation, as well as emphasizing the influence of temperature on the wine fermentation process, a NetLogo simulation of wine fermentation was programmed. The detailed results can be seen in section 3.6 below.

3.1 Wine Tasting Panel Evaluation

The wine tasting panel evaluated the aroma of the wine samples for its detailed ester features such as fruits, white flower, spices, and honey. The samples were separated into a group of 4 samples and a group of 5 samples to ensure accuracy for each round of tasting. The score for each aforementioned feature of the samples in each group was marked on a scale (a straight line with length 95mm on the evaluation sheet). The score for each feature was calculated as follows:

$$Score_{Sample\ 1,Feature\ 1} = \frac{Length\ of\ Sample\ 1\ Mark\ on\ Feature\ 1\ Scale\ (mm)}{Full\ Scale\ Length\ (95mm)} \times 100$$

The scores of all 9 samples given by all 9 judges were then plotted on the dot plots below (Figure 5 – 11). Each figure displayed the scores of all samples for one ester feature.

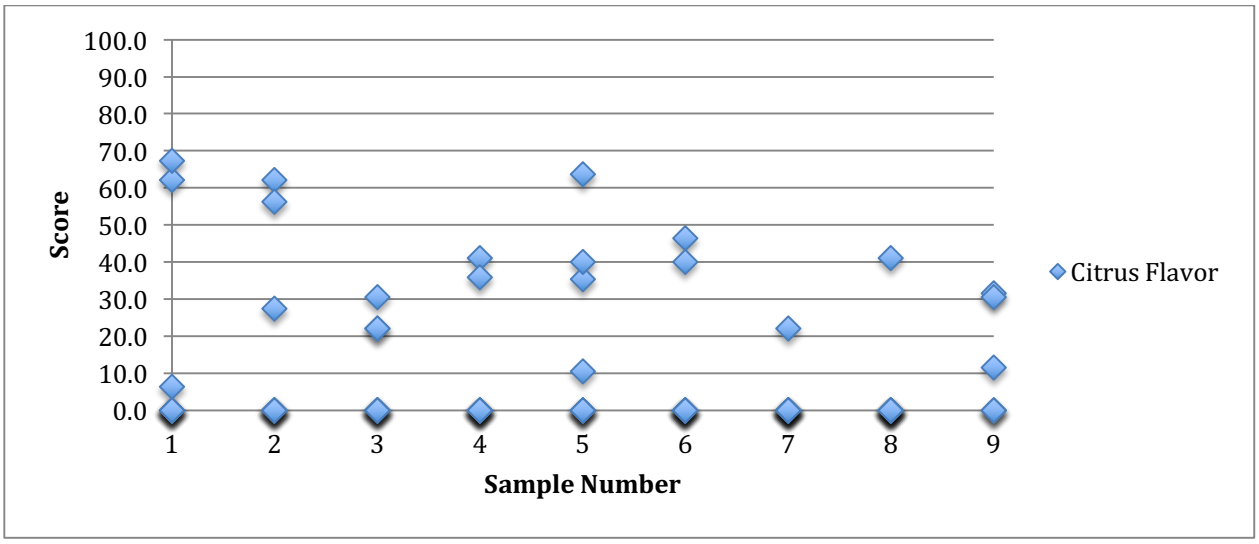

Figure 5: Scores of Citrus Fruit Aroma (Sample 1-9)

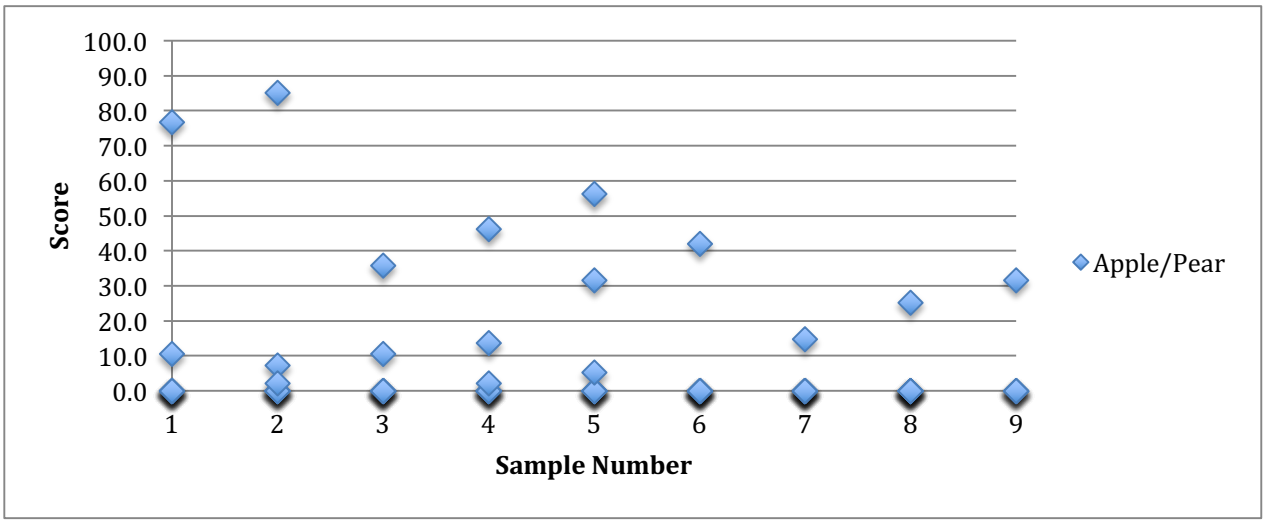

Figure 6: Scores of Apple/Pear Fruit Aroma (Sample 1-9)

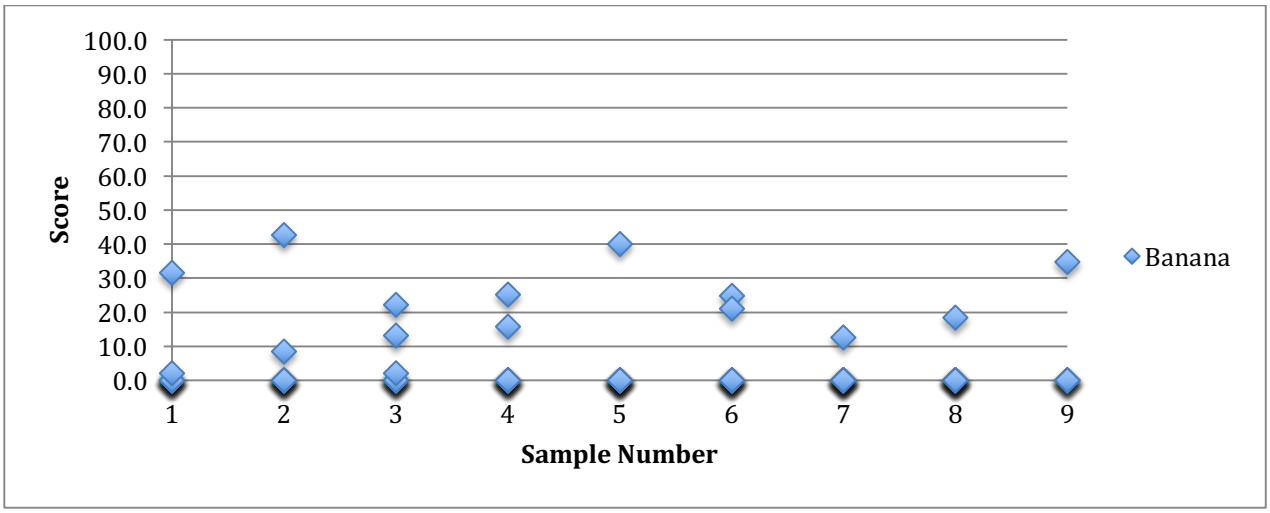

Figure 7: Scores of Banana Fruit Aroma (Sample 1-9)

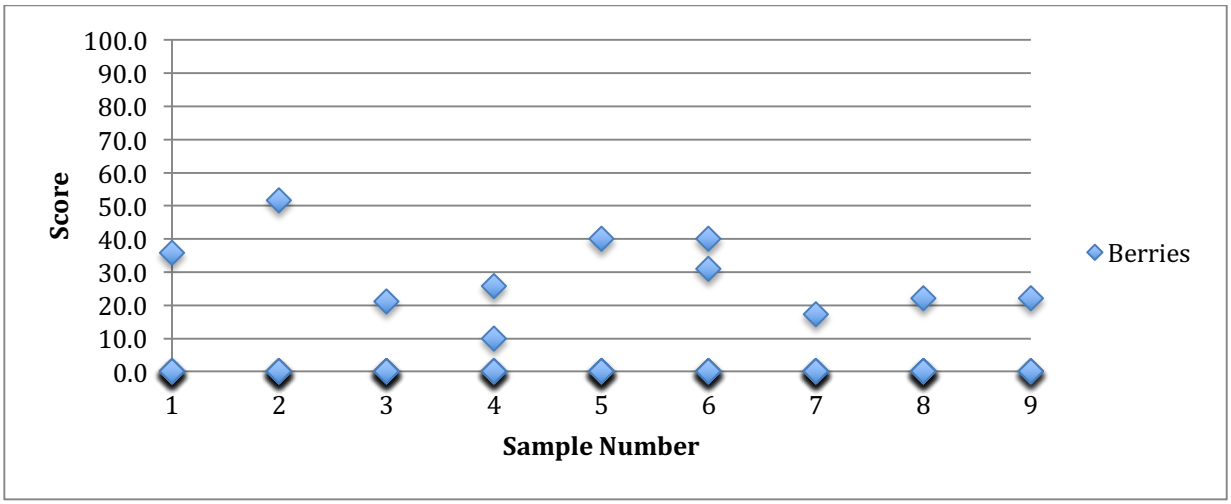

Figure 8: Scores of Berry Fruit Aroma (Sample 1-9)

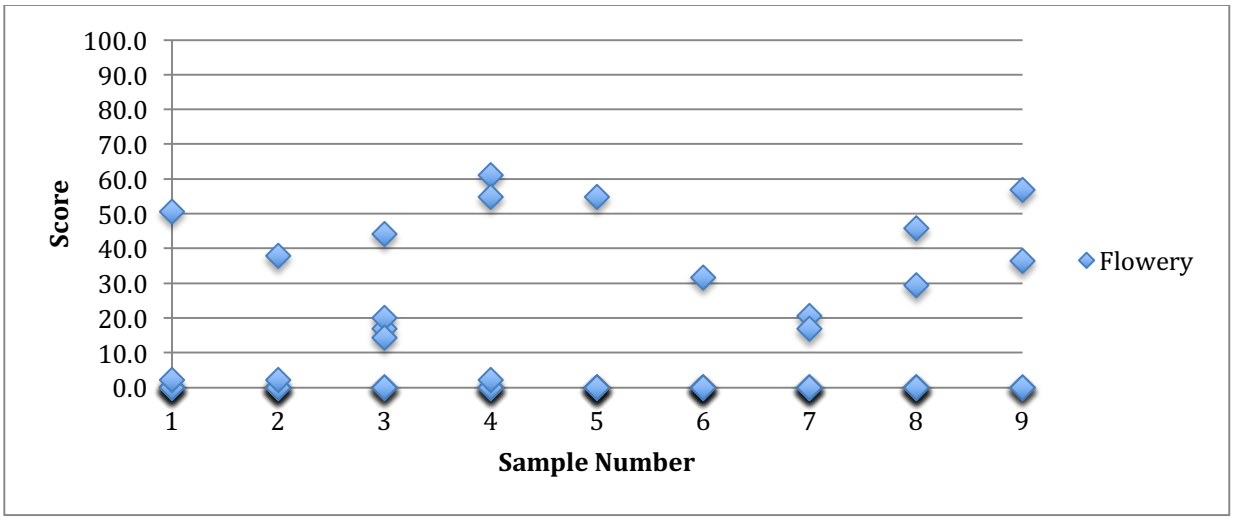

Figure 9: Scores of Flowery Aroma (Sample 1-9)

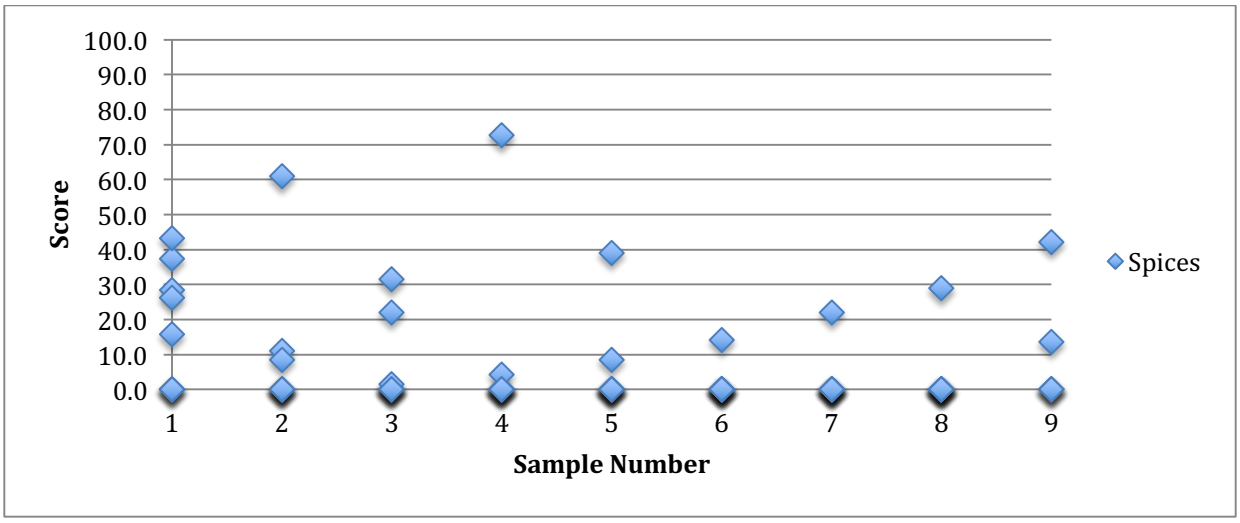

Figure 10: Scores of Spice Aroma (Sample 1-9)

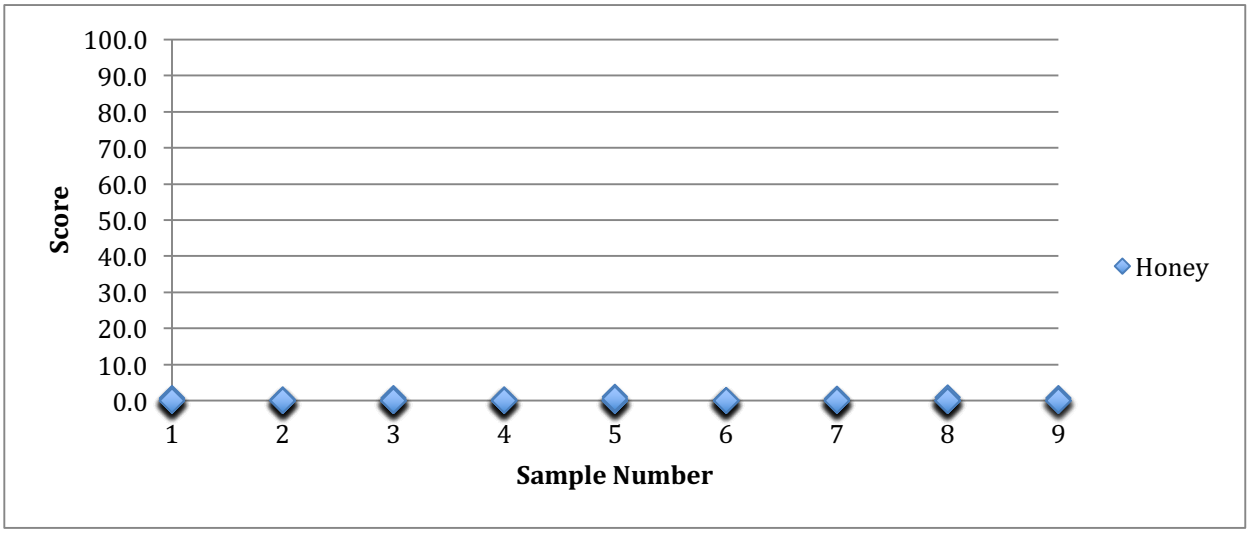

Figure 11: Scores of Honey Aroma (Sample 1-9)

The data in Figure 5 through Figure 11 show that personal perception of the judges to the wine samples varies.

Table 5: Tasting Panel Score Overview, concludes the number of features each sample scored at once higher than the highest score of Sample 1 (Control Conditions)

Sample Number	1	2	3	4	5	6	7	8	9
Number of Aroma Features Scored Higher than Control Sample	N/A	4	0	3	3	1	1	1	4

It can be seen in Table 5 that Sample 2 and Sample 9 both had 4 ester features which were scored higher than these features of Sample 1 at least by one judge. Sample 4 and Sample 5 both had 3 such ester features. These results suggest that the low pH and high nitrogen conditions yielded more ester features in wine aroma than other conditions. They could be applied to grape must in the future to further investigate their market values.

3.2 GC-MS

To quantitatively evaluate the amount of esters being produced in the experimental samples, a gas chromatography-mass spectrometry (GC-MS) was performed on the 9 samples. The standard analytic kit was run on all samples and the major compounds being reported back were:

- 2-Furancarboxylic acid, quality ~ [60 – 90]
- 4H-Pyran-4-one, quality ~ [70 – 80]
- Phenylethyl Alcohol, quality ~ 60

The quality of the predicted substance needs to reach at least 60 to have a reasonable confidence level towards the prediction. The first two compounds on the list appeared in the analytic results of most samples and the phenylethyl alcohol appeared in the results for Sample 8. The gas chromatography peaks were shown in Figure 12 below.

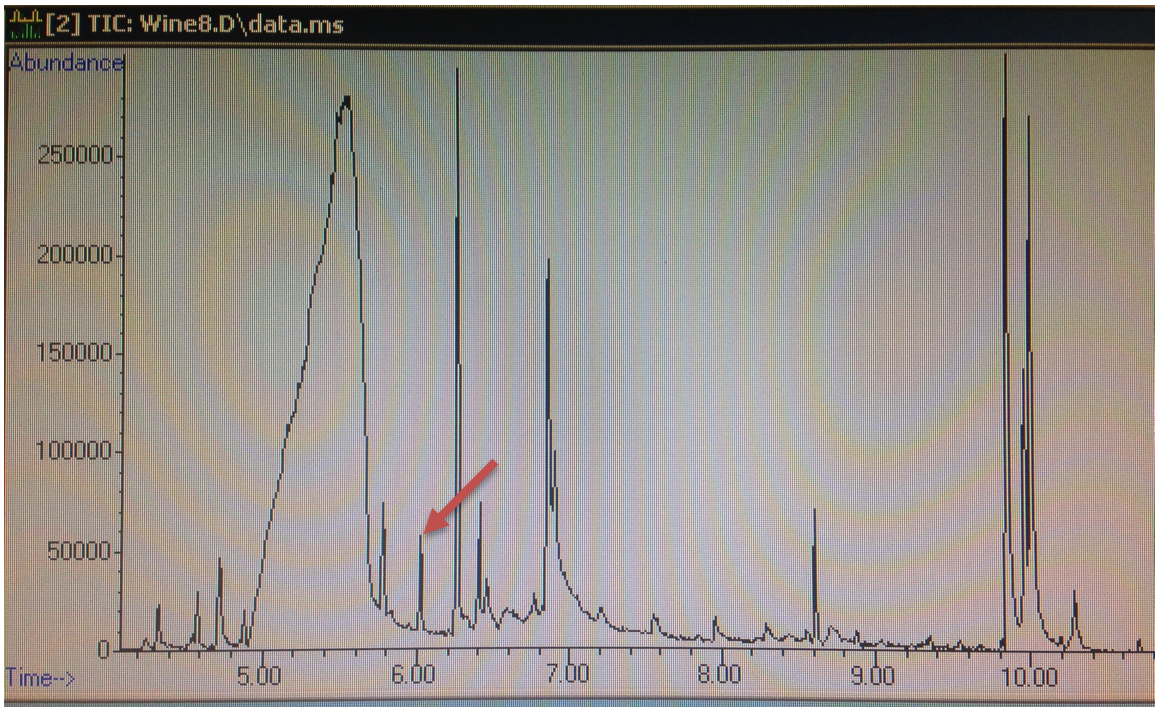

Figure 12: Gas Chromatography (x-axis represents the time point when the chemical was separated from the mixture; y-axis represents the amount of chemical being separated at the same time point/with the same boiling point) - Sample 8, with the phenylethyl alcohol peak pointed out by the red arrow.

Figure 12 showed that the phenylethyl alcohol peak in the gas chromatography analysis was very small, indicating that the phenylethyl alcohol only occupied a very small portion of the total amount of chemicals in the wine sample 8. It was not able to reach the peak height required for the gas chromatography area percent report, so there was no data informing the accurate amount of phenylethyl alcohol in the sample.

Another wine sample gas chromatography analysis done on a grape must fermentation conducted by another Major Qualifying Project on WPI campus (Jia, 2016) was shown in Figure 13 below.

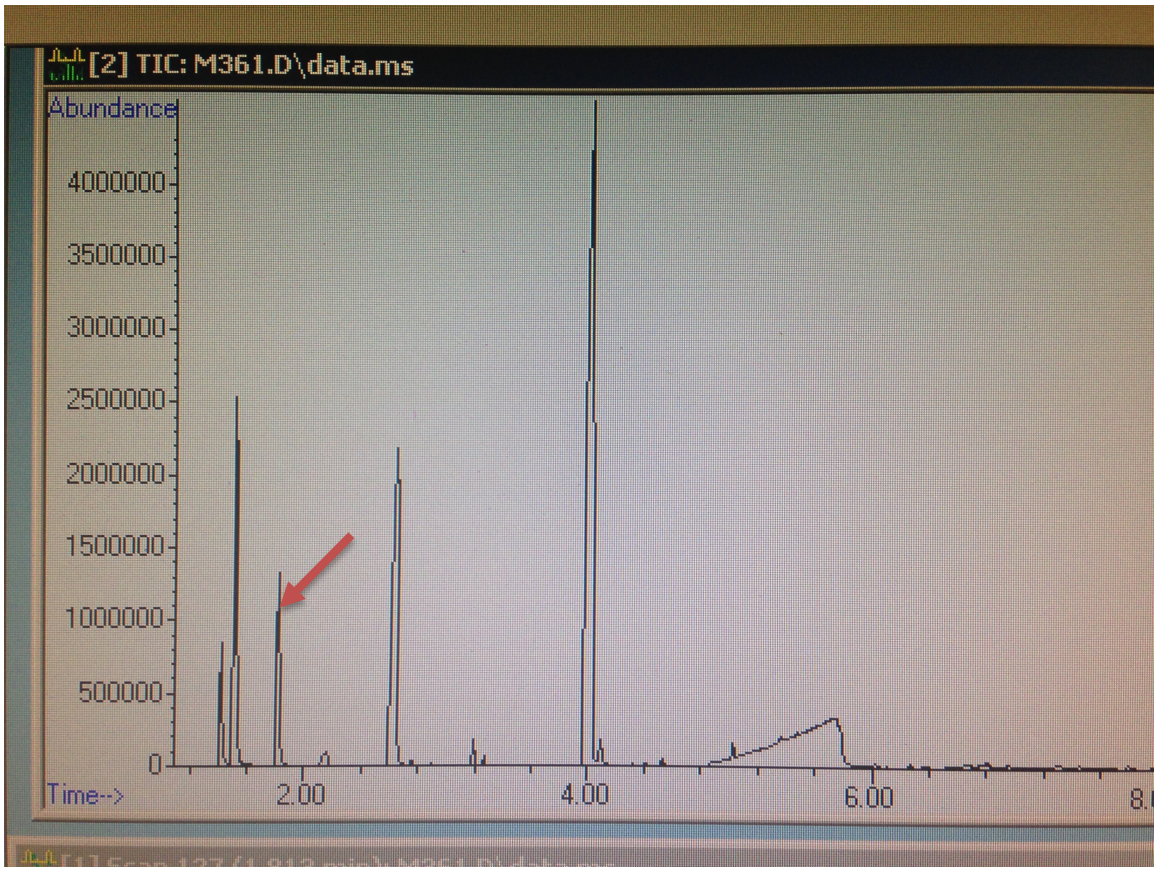

Figure 13: Gas Chromatography (x-axis represents the time point when the chemical was separated from the mixture; y-axis represents the amount of chemical being separated at the same time point/with the same boiling point) - Grape Must Fermentation, with ethyl acetate pointed out by red arrow (Jia, 2016).

It can be seen in Figure 13 that the ethyl acetate (the simplest ester with fruity aroma) was separated out of the wine sample at the time point less than 2 minutes. However, looking back to Figure 14, most amount of chemicals started to be separated from the mixture after 5 minutes.

The gas chromatography analysis results showed that none of the chemicals that were seen in the analysis were related to the common esters identified in wine tasting, suggesting that the samples were degraded before going through the GC-MS analysis.

3.3 RT-PCR

In order to determine the expression level of the ATF2 transcript and its eventual effect on the ester profile, RNA extraction followed by RT-PCR was performed on the yeast

cells when collecting the fermentation flasks. The agarose gel of all samples' RT-PCR products was exposed under UV light and the pictures taken can be seen in Figure 14 below.

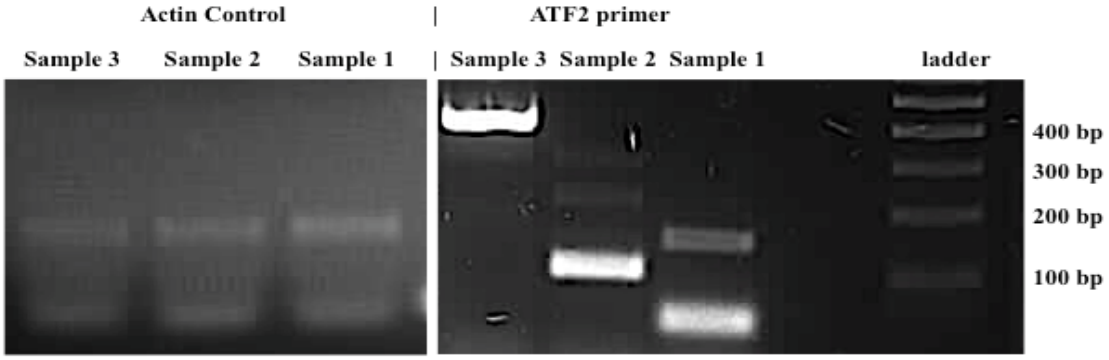

(a)

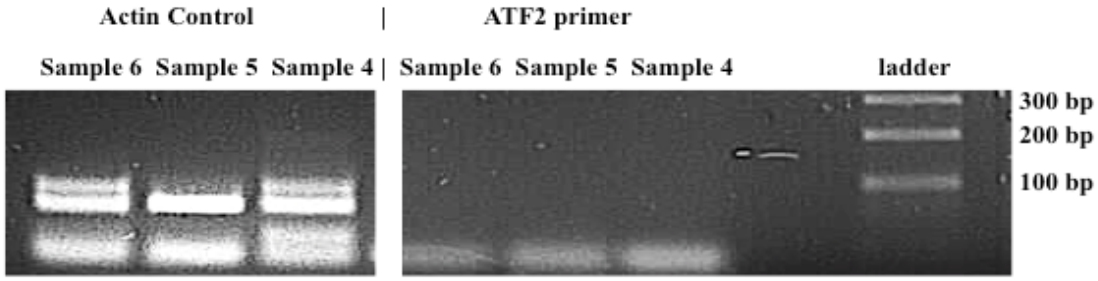

(b)

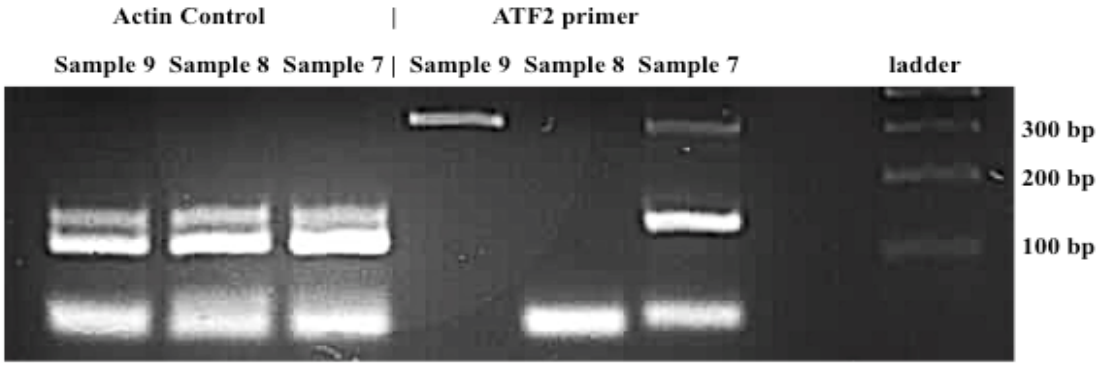

(c)

Figure 14: RT-PCR Product Agarose Gel Electrophoresis (a) Sample 1, 2, and 3 (annealing temperature 57°C, 50 cycles; 90V, 30 minutes, 2% gel), amplicon at ~150bp for Sample 1, ~120bp for Sample 2, and ~400bp for Sample 3; (b) Sample 4, 5, and 6

(annealing temperature 57°C, 50 cycles; 80V, 35 minutes, 2% gel), no amplicon for all 3 samples; (c) Sample 7, 8, and 9 (annealing temperature 55°C, 50 cycles; 90V, 30 minutes, 2% gel), amplicons at ~130bp and ~300bp for Sample 7, no amplicon for Sample 8, and ~300bp for Sample 9.

By comparing the 3 panels of Figure 14 it can be seen that the RNA extraction followed by the RT-PCR procedure was generally successful, indicated by the amplicons given by the actin control groups. However, the sizes of the amplicons coming from the ATF2 primers were not the same as predicted. Sample 3 and Sample 7 had amplicons at the approximately the size of the anticipated ATF2 amplicon length (322bp), while other samples either had no amplicon at all or weak and/or strong signals at other lengths.

3.4 Bradford Assay

A Bradford Assay was performed on yeast cell samples of equal amount taken from each fermentation flask. This was done to investigate any changes on the overall amount of protein in yeast cells due to the fermentation condition variations. The calculated protein concentration of all flasks can be seen in Table 6 below.

Table 6: Calculated Protein Concentration for All Flasks

Sample	Calculated Protein Concentration (mg/mL)
1	0.095
2	0.060
3	0.062
4	0.076
5	0.097
6	0.081
7	0.109
8	0.087
9	0.083

It can be seen in Table 6 that comparing to control sample 1, sample 5 and 7 had slightly higher protein concentration, while all other samples had slightly lower protein concentration. However, the Bradford assay results only indicated differences among the overall protein levels of the 9 samples being assayed in one run. The difference cannot be quantitatively evaluated since there was no other wine-fermenting yeast overall protein data to compare with. The experiments were not replicated enough times either to provide any statistical significance.

3.5 Bioinformatics

3.5.1 Protein Sequence Alignment

To compare and contrast the alcohol O-acetyltransferases (AATs) encoded by the ATF2 gene in different wine fermenting yeast strains, the protein sequences for AAT of two strains, S288c and EC1118, were aligned and compared. The protein sequences were aligned with NCBI Protein-BLAST (Figure 13). The sequences were aligned with a score greater than or equal to 200, which was anticipated for two strains of the same species.

Figure 15: Comparison of the AAT protein sequence in EC1118 and S288c taken from NCBI Protein-BLAST results. The red dots showed the two mismatched amino acid residues found in the alignment. (NCBI, 2016)

Figure 15 showed that there are only 2 protein mismatches in the AAT protein from the two strains, shown by the red dots in the final panel. The figure supported that the protein sequences are very similar to each other in the two subject strains.

3.5.2 Protein Structure Predictions and Comparison

To determine if the structure of the AAT enzyme varies from strain to strain, the protein structure was predicted and modeled. ModBASE was the database that provided a model for the target protein sequence. ModBASE uses the ModPipe software to calculate comparative models for the query sequence with no manual intervention (Pieper et al., 2004). It was noted that the model provided by ModBASE had a percent identity of 18%, which indicates the model may not be very accurate, since conventionally a good model has a percent identity higher than 30%. MODELLER was used to predict the structure of AAT in both strains. UCSF Chimera was used to produce the images in Figures 16.

*Figure 16: Superimposition of predicted alcohol O-acetyltransferase (AAT) structures for strain S288c (shown in tan) and strain EC1118 (shown in blue).*This graphic was obtained from UCSF Chimera (2016) and the data used to generate this graphic was obtained from MODELLER (2016).

Figure 16 showed that most secondary structures of the two structures for alcohol O-acetyltransferase were similar. However, the superimposition was not as good due to inconsistences in the loop sections.

To further investigate whether the point difference shown in the protein sequence alignment (Figure 15) had any influence on the structure of the protein, the two point differences were highlighted in the superimposition (Figure 17). The highlights can be seen in Figure 17 and Figure 18 below.

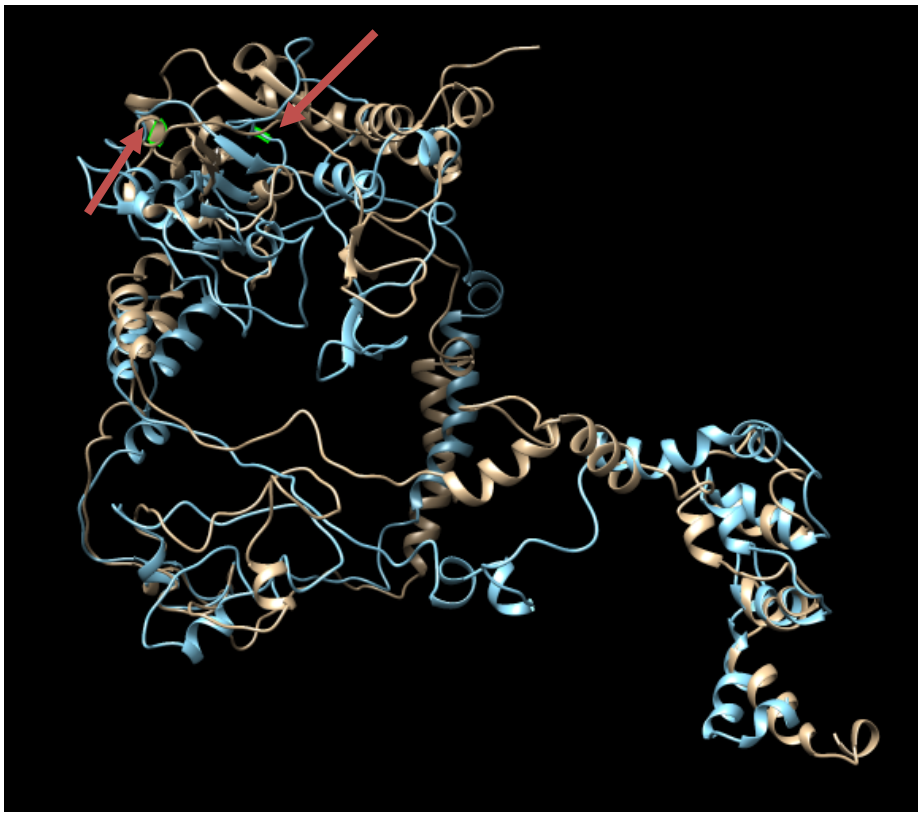

*Figure 17: Superimposition of predicted alcohol O-acetyltransferase (AAT) structures for strain S288c (shown in tan) and strain EC1118 (shown in blue) with #435 mismatched amino acid residue highlighted in green (also marked out by red arrows).*This graphic was obtained from UCSF Chimera (2016) and the data used to generate this graphic was obtained from MODELLER (2016).

It can be seen in Figure 17 that the mismatched position was a part of an alpha helix in the ATF2 structure strain S288c and a part of a loop in the ATF2 structure of strain EC1118.

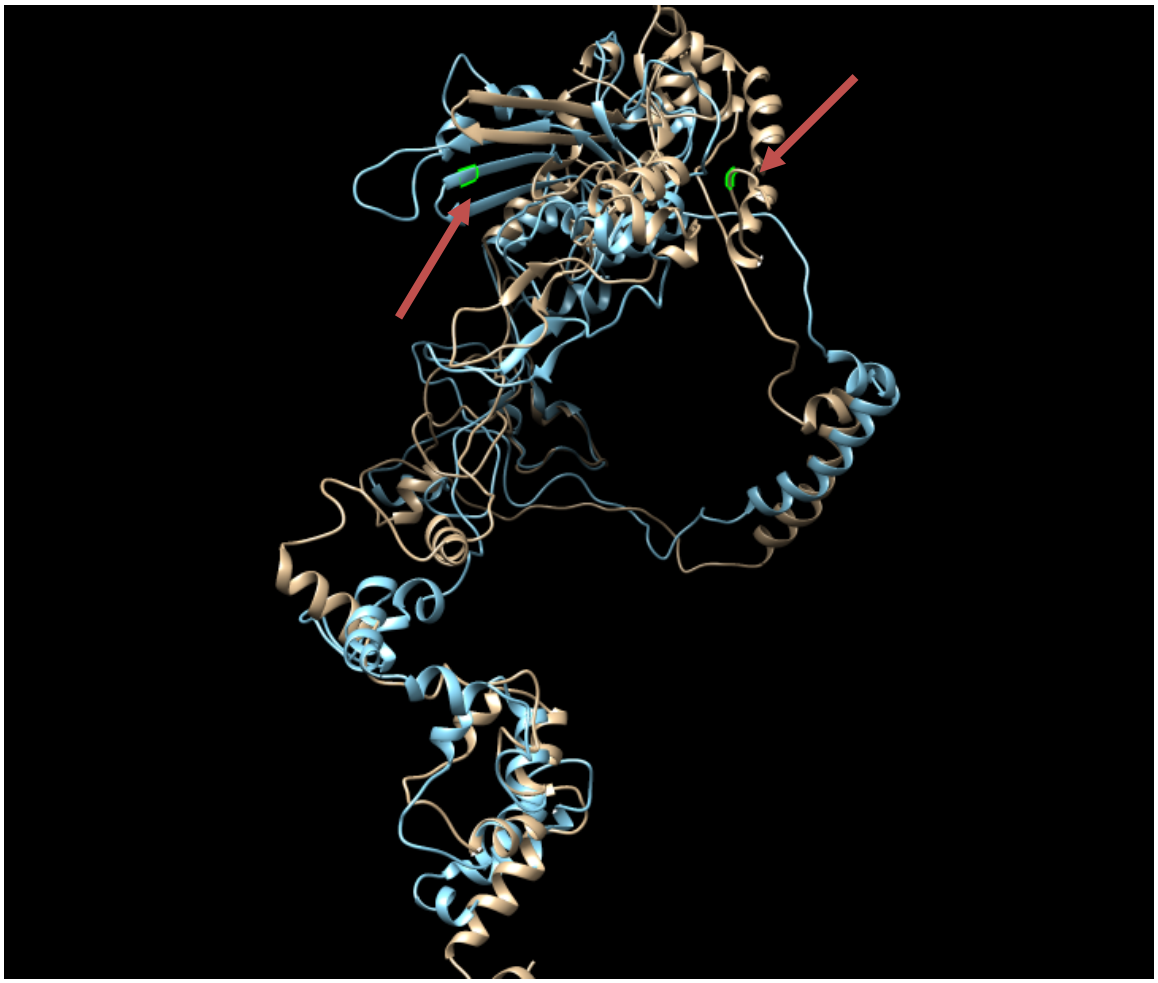

*Figure 18: Superimposition of predicted alcohol O-acetyltransferase (AAT) structures for strain S288c (shown in tan) and strain EC1118 (shown in blue) with #530 mismatched amino acid residue highlighted in green (also marked out by red arrows).*This graphic was obtained from UCSF Chimera (2016) and the data used to generate this graphic was obtained from MODELLER (2016).

It can be seen in Figure 18 that the mismatched position was a part of a loop in the ATF2 structure of strain S288c but a part of a beta pleated sheet in the ATF2 structure of strain EC1118. These results suggest that the amino acid changes may have some effect on the secondary structure of the protein.

3.5.3 Phylogenetic Tree

To observe the genetic distance between the strain S288c and strain EC1118 with regard to the ATF2 gene, a phylogenetic tree was generated through SGD. It can be seen in Figure 19 below.

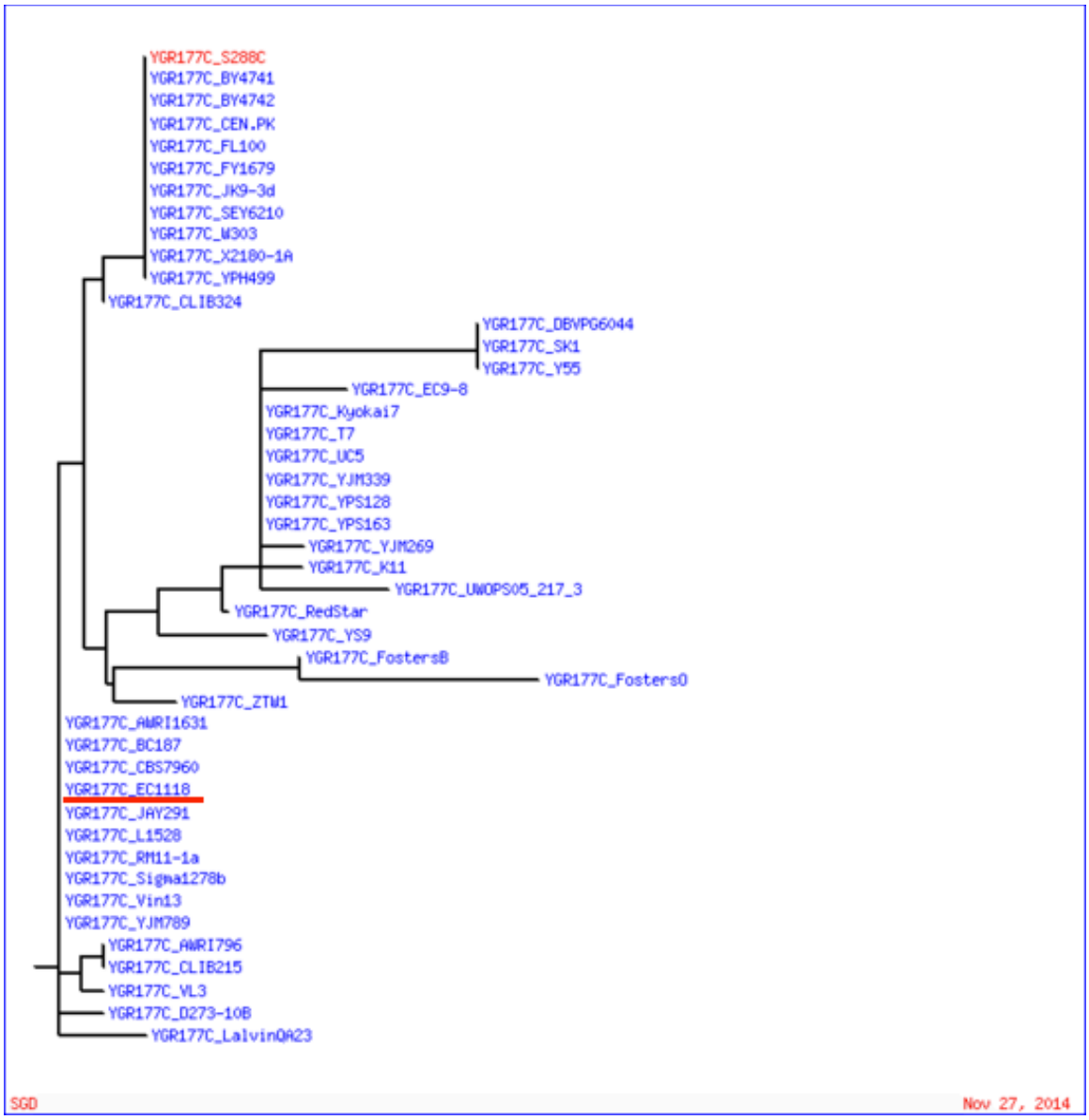

Figure 19: Phylogenetic tree of 45 strains in SGD (SGD, 2014), with strain S288c shown in red, and strain EC1118 underlined in red.

It can be seen in Figure 19 that the genetic distance between strain S288c and strain EC1118 with regard to the ATF2 gene was relatively far away. Since the tree was built comparing different yeast strains instead of comparing yeast and other species, the strains with regard to the ATF2 gene might seem far away from each other, but the actual sequence differences between the strains were small. For instance, strain BY4741 was the closest to the lab strain S288c, and these two strains were identical both when comparing

the ATF2 coding DNA sequence and the ATF2 translated protein sequence. There were 2 point differences between the ATF2 protein sequences of the two strains in the multiple sequence alignment shown in Figure 15, therefore the two strains were far away from each other on the phylogenetic tree.

3.6 NetLogo Wine Fermentation Simulation

In order to provide insight on the ethanol and ester level of the commercial red wine, as well as demonstrating the molecular interactions among chemical molecules and yeast cells in wine fermentation, a NetLogo simulation was programmed. The simulation contained two views: the wine view, which demonstrated the wine fermentation process outside of the yeast cells in the grape must mixture; and the yeast view, which demonstrated the wine fermentation process inside of a yeast cell.

3.6.1 Wine View

Figure 20 below shows the initialization of the fermentation process outside of the yeast cells in wine must, where the color of the mixture had been determined by cold soaking the mixture under the correct temperature and the yeast cells had been added to the grape must mixture, ready to interact with the glucose molecules in the must. The fermentation temperature slider on the left hand side can be used to control the temperature applied to the fermentation environment, which would change the speed of the molecule movement, and was expected to change the speed of the reaction as well. The fermentation temperature would also influence the growth rate of the yeast cells in wine.

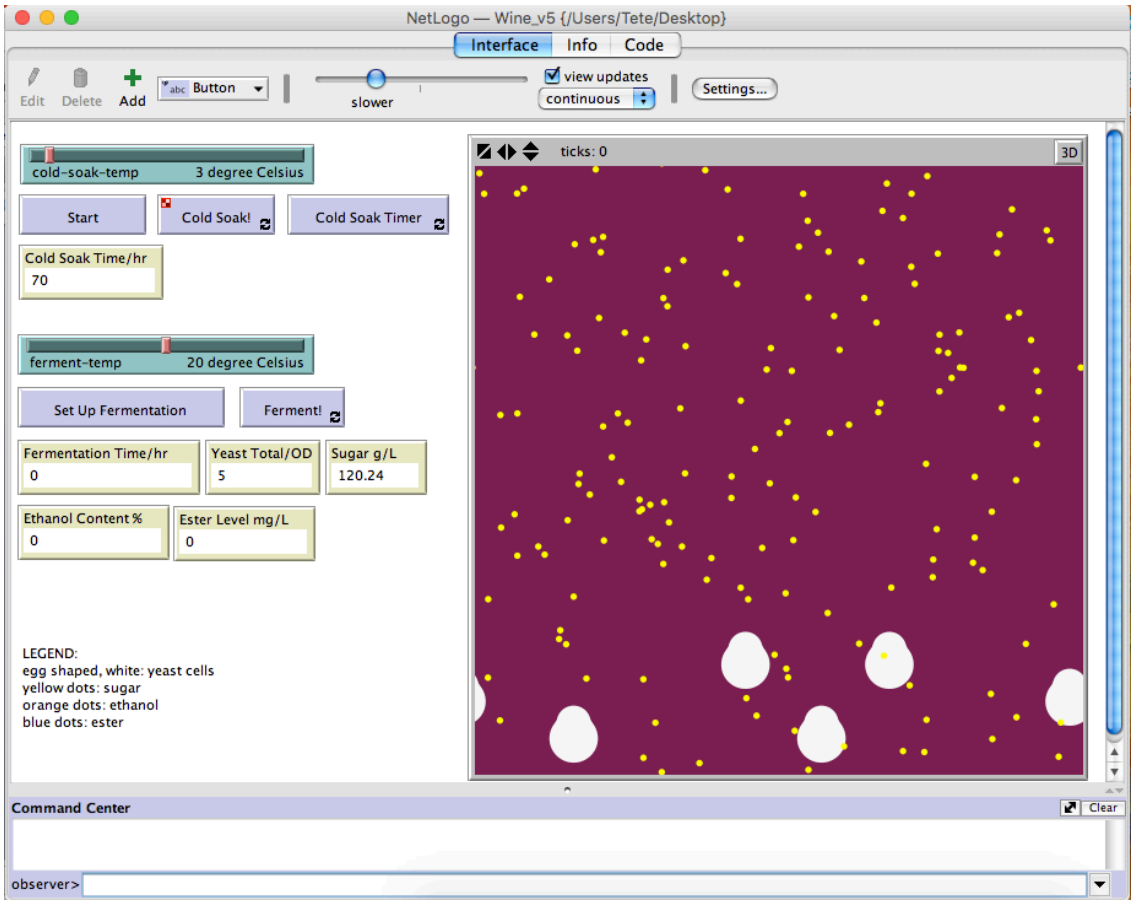

Figure 20: NetLogo simulation: wine view fermentation initialization. The background color was formed after running the cold soak function under soaking temperature lower than 10 degree Celsius. The small yellow dots on the canvas represent sugar molecules (one dot represented 1 mmol of glucose), and the big egg-shaped agents represent yeast cells (one agent represented 1 OD unit of yeast cells).

The monitors in the simulation had different measuring units (Figure 20). The monitors counted the amount of each type of agent in the environment and did the calculation for the users to convert number of agents to the most common measuring unit for that type of agent. For instance, it is very common for people to understand the amount of ethanol in existence of a bottle of wine through its ethanol volume percentage.

The model had each chemical agent represent 1 mmole of such chemical to simplify the amount of calculation needed to be done for this simulation model. Each collision of one glucose agent (yellow dot) with yeast cells (white egg-shaped agent) would create an ester agent in a 1:90 chance. Otherwise the collision would create ethanol agents (orange

dots). This was to model the number disparity of alcohol dehydrogenases and alcohol O-acetyltransferases inside of yeast cells.

Figure 21 below shows the final stage of the simulation when the amount of glucose in the solution had dropped under 7.2 g/L (10 mmole in total), which indicated that the fermentation process was manually stopped at the desired sweetness level and the wine was collected at this point.

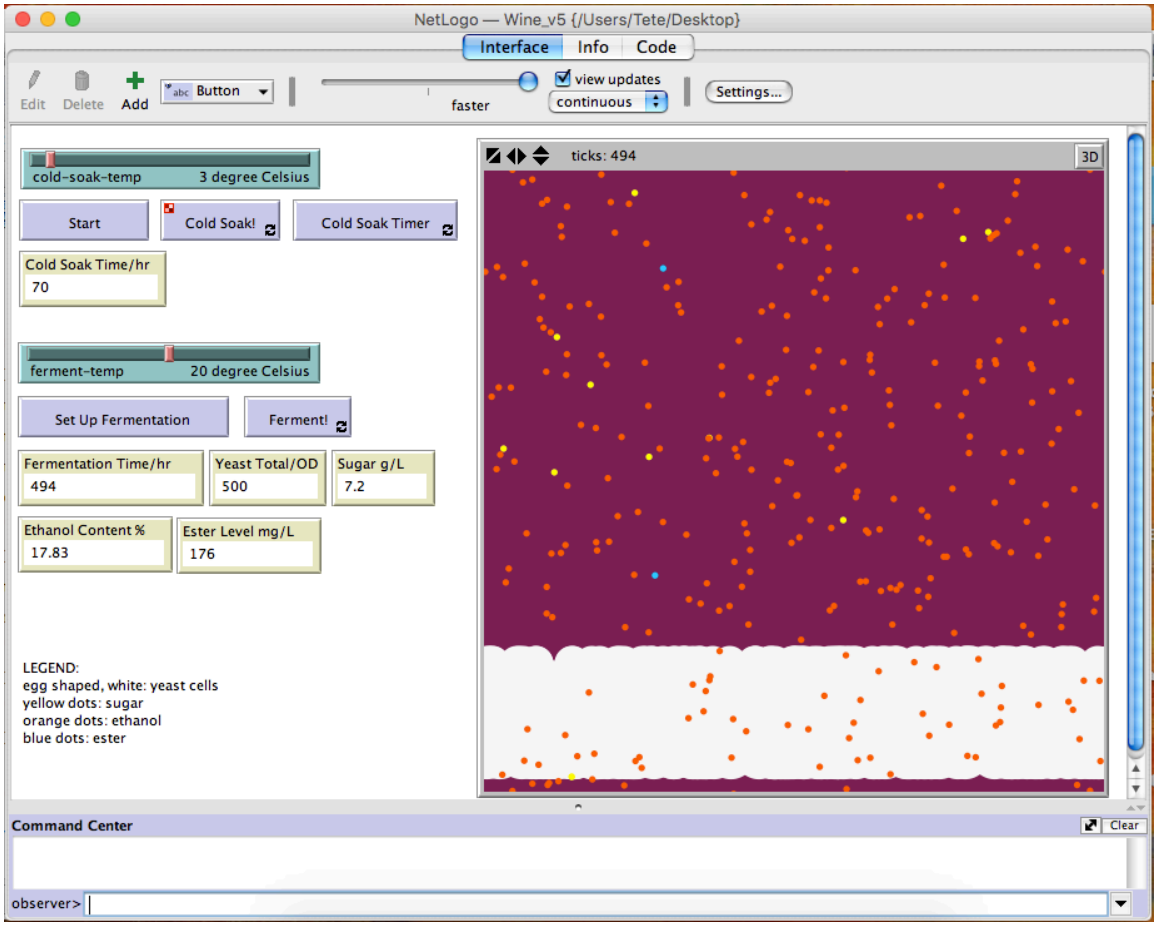

Figure 21: NetLogo simulation: wine view fermentation final stage. The background color stayed the same indicating that the wine color stayed more or less the same during the fermentation process. The number of the yeast cells increased over time and had covered the bottom of the simulated fermentation flask (white). The amount of glucose (yellow dots) was reduced over time due to consumption by the yeast. The ethanol (orange dots) and esters (blue dots) were produced by fermentation over time.

It can be seen in Figure 21 that the fermentation process had gone through 494 hours, with a final yeast amount of 500 OD (A590), glucose level of 7.2 g/L, a final ethanol

level of 17.83%, and a final ester level of 176 mg/L. These numbers were consistent with the data obtained from common red wine samples.

3.6.2 Yeast View

Figure 22 below showed the initialization of the fermentation process inside of the yeast cells in wine must, where the color of the mixture had been determined by cold soaking the mixture under the correct temperature and the yeast cells were ready to interact with the glucose molecules in the must. The fermentation temperature slider on the left hand side can be used to control the temperature applied to the fermentation environment, which would change the speed of the molecule movement, and was expected to change the speed of the reaction as well.

On the other hand, for the AAT enzyme, in reality it has a 90 to 1 amount disparity comparing to the alcohol dehydrogenase. To ensure that the amount of ester/ethanol being produced is correctly simulated and to make the canvas not overly crowded, the number of the AAT enzyme and alcohol dehydrogenase was set to a 1:9 ratio. On top of that, a pyruvate agent is catalyzed into an ethanol agent upon encounter with an alcohol dehydrogenase, but is only catalyzed into an ester agent in a 1:10 chance upon encounter with an AAT enzyme. The 90 to 1 amount disparity was then simulated.

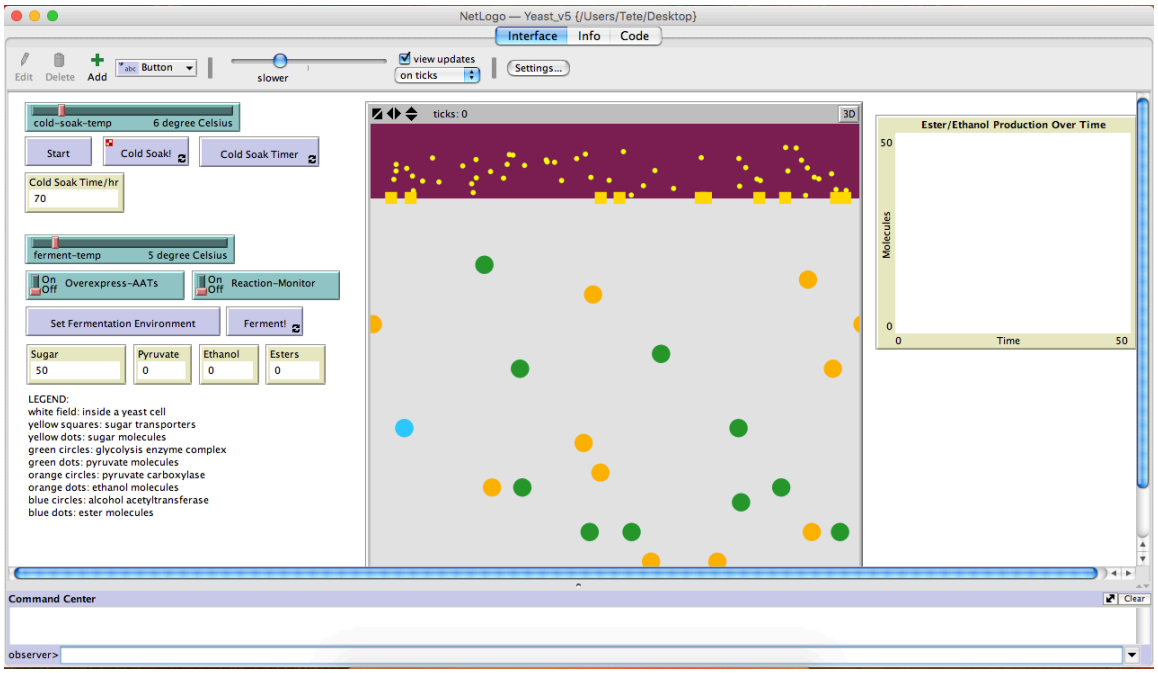

Figure 22: NetLogo simulation: yeast view fermentation initialization. The inside of the yeast cell was colored grey and the outside environment had gone through the cold soak process and was advanced to red wine color. Glucose molecules (yellow dots) were located at random in the outer environment. The membrane of the yeast cell was guarded by sugar transporters (yellow cubes). The glycolysis enzyme complex (green circles), alcohol dehydrogenase (orange circles), and alcohol acetyltransferase (blue circle) were located at random inside of the yeast cell.

Figure 23 below shows how the visualization looked like in the middle of one run. In this model, the number of ticks does not correspond to the actual number of hours spent for fermentation since its major function was to demonstrate the cellular and molecular interactions happening inside of the yeast cell. The reactions being demonstrated were:

- Glycolysis
- Initiation of Citric Cycle (pyruvate to acetyl-CoA)
- Esterification of higher alcohols

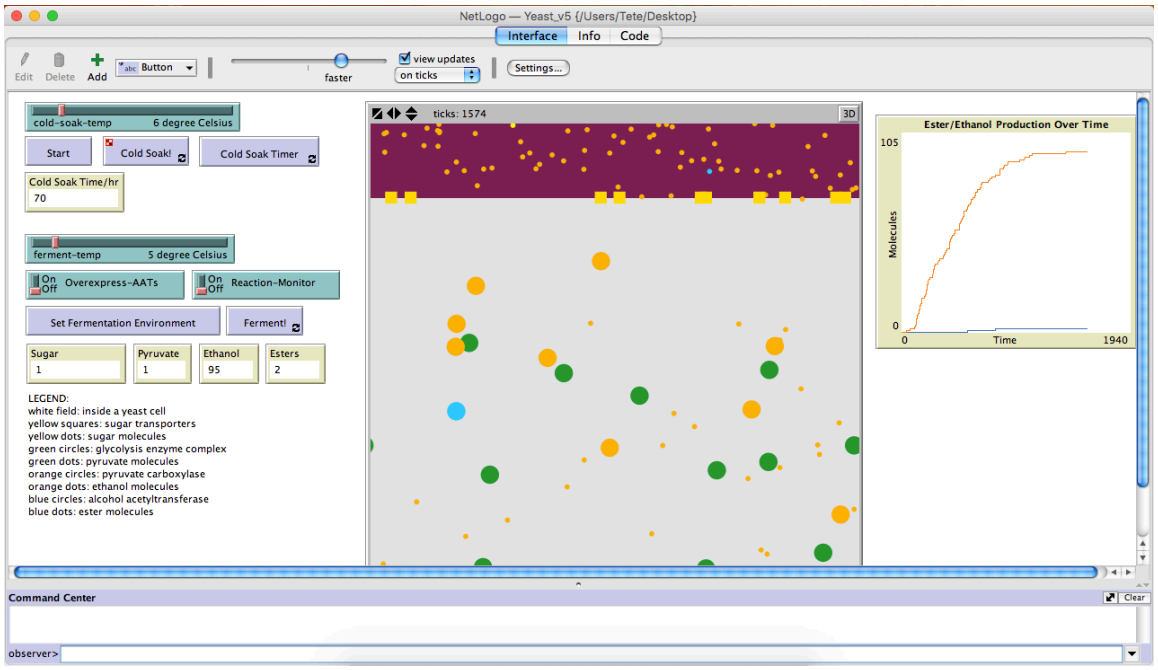

Figure 23: NetLogo simulation: yeast view mid-progression with normal AAT level. The produced ethanol (orange dots) and esters (blue dots) had mostly diffused outside of the yeast cells.

The model can be modified to overexpress the AAT enzymes inside of the yeast cell. In addition, the user can switch on the reaction monitor mode to observe the whereabouts of the glucose agent before and after interacting with a glycolysis enzyme complex.

Ester production was very minor comparing to ethanol production when the AAT enzyme expression level was normal (Figure 23). Figure 24 below showed how the resulting graph looked if the AAT enzyme was overexpressed.

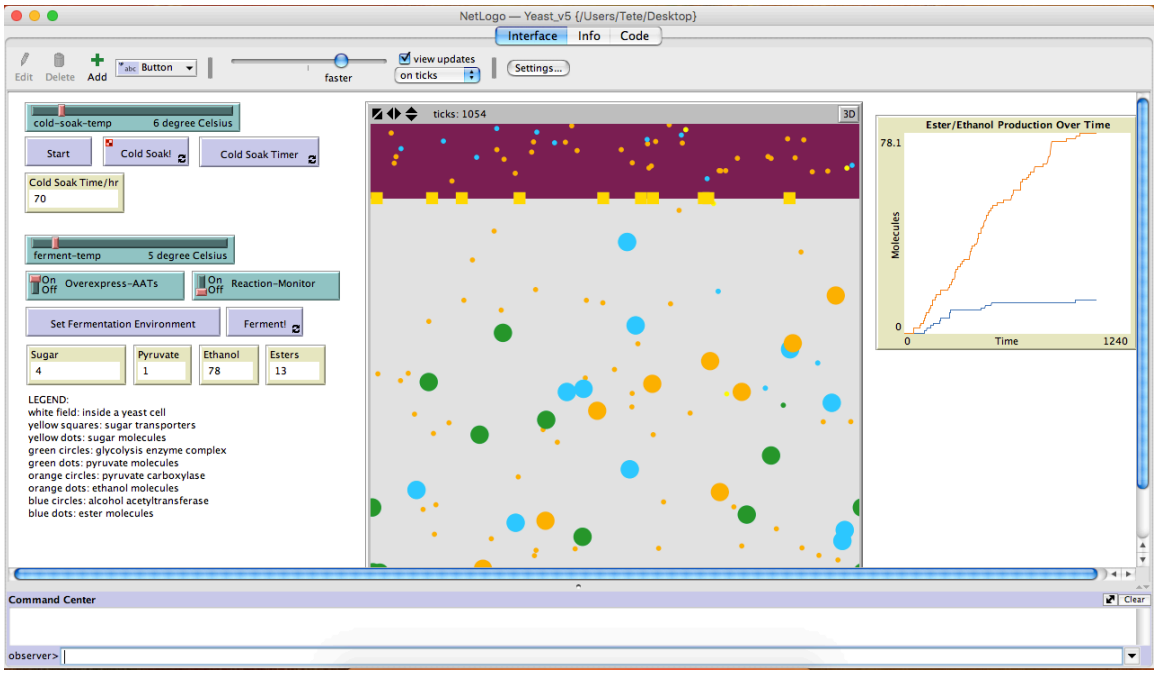

Figure 24: NetLogo simulation: yeast view mid-progression with overexpressed AATs. The produced ethanol (orange dots) and esters (blue dots) had mostly diffused outside of the yeast cells.

It can be seen in Figure 24 that there were much more esters produced with the assistance of the increased number of AAT enzymes. To supplement the graphical presentation of data, the monitors on the left hand side provide an exact count of how many agents were produced/presented on the canvas.

To better demonstrate the chemical reactions happening upon contact with the yeast enzymes, a reaction monitor mode was implemented into the model. By switching on the Reaction-Monitor switch, the glucose molecules (yellow dots) that come in contact with the glycolysis enzyme complex (green circles) will turn dark brown and keep moving in the environment. The monitor mode will only show the users the "deletion" of glucose agent and the creation of pyruvate agents, therefore the "deleted" glucose agent (dark brown) will not be able to interact with glycolysis enzyme complex agents in the environment. Figure 25 below demonstrated the simulation view when the Reaction Monitor was on.

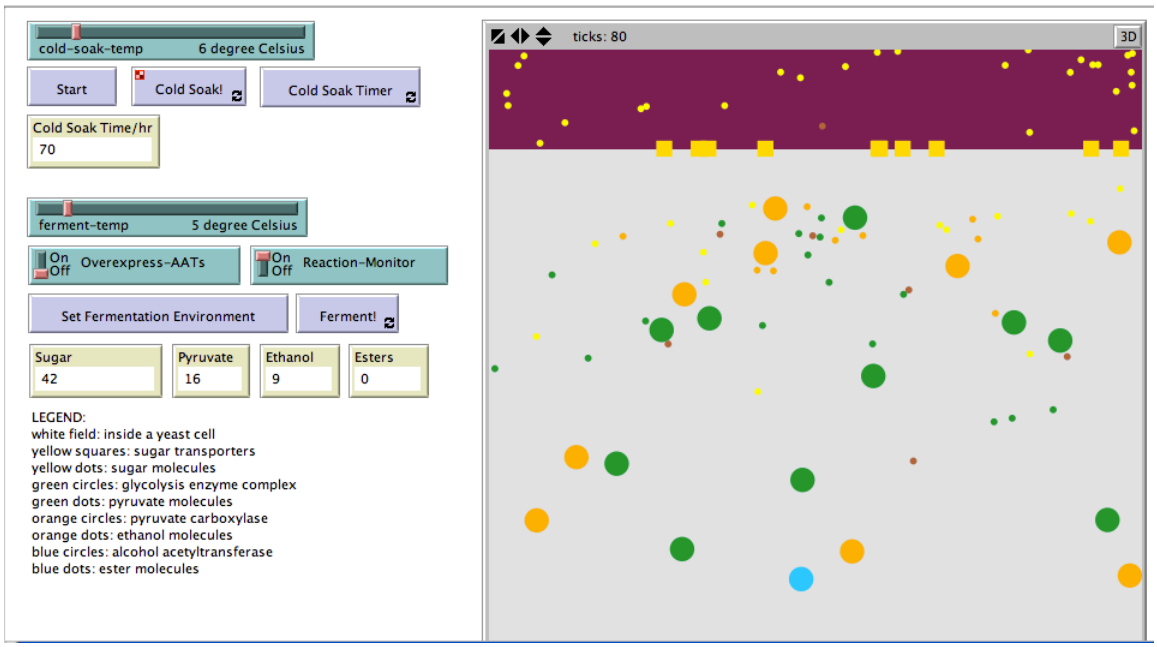

Figure 25: NetLogo simulation: yeast view mid-progression with Reaction Monitor on. The glucose (yellow dots) came in contact with the glycolysis enzyme complex (green circle) turned dark brown instead of being deleted so that the users were able to understand the agent interaction mechanism behind the simulation thoroughly.

4. DISCUSSION

We investigated the relationship between the expression of ATF2 gene in yeast and the ester profile in wine aroma, via both a wine production approach and an agent-based modeling approach.

4.1 Evaluation of Fermentation Regarding ATF2 Gene Transcription and Translation

The ATF2 gene translates to alcohol O-acetyltransferase (AAT) enzyme in yeast, which catalyzes the esterification of higher alcohols in yeast and contributes to the ester aroma in wine. We took the wine production approach in wet lab to see if altering the wine fermentation conditions, such as pH value, fermentation temperature, glucose/fructose ratio, and nitrogen content, would influence the expression level of the ATF2 gene, and further influence the ester profile of wine aroma. The expression level of the ATF2 gene was evaluated at the transcriptional level through RT-PCR, translational level through Bradford Assay, and ester production level through the evaluation of a professional wine tasting panel and a GC-MS analysis.

The RT-PCR results were able to associate ATF2 gene transcription level with some fermentation conditions. It was hypothesized that the more acidic (lower pH) the environment was, the more substrate there is for ester production pathway, and the faster the ester production pathway would progress. However, the RT-PCR results suggested that both the higher and lower pH level environments increased the transcription of the ATF2 gene. It was hypothesized that a higher temperature would be able to increase the transcription of genes since yeast cells would be more active under higher temperature. However, the RT-PCR results did not provide evidence to support this hypothesis. The ATF2 transcription level was increased under high glucose condition, which provided some evidence to support the hypothesis that higher glucose concentration would yield higher ester production since glucose is easier for yeast cells to take in as food comparing to fructose. In particular, the ATF2 gene had a higher transcription level at high nitrogen environment. The results provided some evidence to support the hypothesis that the high

nitrogen level is a more comfortable environment for yeast to grow, so that the transcription activities would be more active. However, the results would need to be replicated at least three times before strong conclusions could be reached.

The Bradford assay was a preliminary assay, used in place of a western blot targeting AAT enzyme translated directly from ATF2 gene. It was not budgeted for the project to purchase an AAT specific antibody to perform the western blot. Instead, a Bradford assay was done to investigate overall protein level up-regulation/down-regulation under various fermentation conditions. The results suggested that comparing to the control condition, high temperature conditions and high glucose conditions had higher overall protein content in a fixed amount of yeast cells. This provide some evidence to support the hypotheses that higher temperature and higher glucose content are more friendly environment for yeast cell growth. However, the Bradford assay results can only provide evidence to differences of the overall protein levels among the 9 samples being assayed. The difference cannot be qualitatively evaluated since there was no other wine-fermenting yeast overall protein data to compare with. Also, the assay was only run once on one yeast sample of each fermentation flask. The assay was not replicated enough times to provide any statistical significance. The protein extraction procedure could also cause variability in the results.

Overall for the wet lab assays, the RNA/protein extraction procedures prior to the assays were done using mechanical grinding of yeast cells with glass beads. This method could have caused a lot of the RNA/protein being discarded with the beads, comparing to chemical extraction procedures assisted by instruments. This could have caused the low signals in RT-PCR gels as well as the low protein levels in Bradford assay. In addition, both assays need additional replication trials on the same material to give any statistically significant results.

4.2 Evaluation of Fermentation Regarding Market Value and Precise Ester Content

The tasting panel evaluation of wine samples and the GC-MS analysis done over the wine samples were designed to evaluate the ester production in wine fermentation both in the aspect of human perception and the aspect of scientific analysis.

Since the wine was fermented on artificial must, and since the esters are detected by smell rather than taste, the tasting panel only smelled the samples but did not taste them. It can be seen from the tasting panel figures (Figure 5-11) that most of the judges were not able to detect strong ester features in the wine samples, except for some of the more experienced degustators. It was commented by the tasting panel that since the wine was produced based on artificial wine must, the smell of protein (yeast cells being the major contributors) was very strong and masked most of the ester features. The tasting panel results only suggested that there was potential for some fermentation conditions to yield strong ester profile, but the potential cannot be confirmed until the conditions are eventually applied on grape must-based wine fermentation.

The GC-MS analysis results did not show any signs of ester presence in the samples. This may have been caused by several reasons. Firstly, the analysis was done 2 months after the wine samples were shipped back to WPI campus. During this period of time the samples were defrosted/re-frosted for several times and were not always under -20°C wine sample storage temperature. This could have caused ester degradation in the wine samples. Secondly, esters are generally volatile, and could have been released from the wine sample over such long period of time. Thirdly, since there was no standard wine sample to determine the most appropriate GC-MS analysis procedure, the standard GC-MS procedure was selected. The standard procedure was not able to detect molecules that are lighter, with molecular weights closer to that of water. Furthermore, the most common and simplest form of ester, ethyl acetate, naturally exists in large quantities in grapes. Conducting the fermentation using artificial must with no aromatic compounds to start with could be another reason why the fruity ester aroma was not profound in the products. In Sample 8 the presence of phenylethyl alcohol was detected by GC-MS, which was the only chemical compound detected with fruity smell. Phenylethyl alcohol is

a higher alcohol that could potentially go through esterification and produce esters. It could also contribute to the aroma profile of the wine by itself. However, the project was focusing on the ester related wine aroma, so the presence of phenylethyl alcohol did not provide too much support to the project goal. Moreover, the amount of phenylethyl alcohol detected in Sample 8 was less than 1% (not enough to be shown on the gas chromatography area report). Phenylethyl alcohol could have degraded over the long period of time as well.

4.3 NetLogo Simulation and Wine Fermentation

Wine production and innovation is a big industrial and scientific research field in Slovenia. The Wine Research Center of University of Nova Gorica in Slovenia would like to implement a visual teaching tool to their classrooms to demonstrate abstract biological pathways happening inside of wine must mixture and yeast cells during the wine fermentation process. We were able to develop a NetLogo simulation of the wine fermentation, in both the macroscopic wine fermentation view and the microscopic yeast view, to demonstrate the influence of temperature change on wine fermentation, as well as the effect of ATF2 gene overexpression to ester profile in wine aroma.

The wine view demonstrates how the glucose interacts with yeast cells in wine and produces ethanol (major alcohol content) and ester (major aroma content). It was hypothesized that if the glucose molecules interact with the yeast cells following the guidance of the theoretical biochemical pathways and started with an amount that is common for red wines, the final production of ethanol and esters would be close to the common value for red wines. The simulation simplified the biochemical processes, so that the glucose agent colliding with a yeast cell would produce the appropriate amount of ethanol and esters, following the given amount of molecules going through the biochemical pathway. Each individual agent was represented 1 mmole of a particular type of molecules, such as glucose, ethanol, and esters. Then the amount of each molecule in the fermentation environment was read from the simulation and displayed on the monitor in units that would be most familiar to the user, such as alcohol volume

percentage for ethanol and so on. The final results given by the wine view in Figure 21 supported the hypothesis.

The yeast view, on the other hand, demonstrated molecular interactions occurring inside yeast cells. The amount of initial glucose was set up in a way that it takes some time for all of the agents to be participating in a reaction so that the users are able to observe the progression of the reaction for an extended amount of time. However, this time does not correspond to actual fermentation hours in anyway. The amount of glycolysis enzyme complex and alcohol dehydrogenase in the environment was set up so that their amount ratio is close to their actual amount ratio in yeast cells, yet still leaves room on the canvas for the users to observe the reaction occurring.

The simulation only considered a simplified biochemical pathway of ethanol and ester production. Its limitations include only considering one aromatic compound that contributes to the wine aroma profile, as well as generalizing all ester products as one entity. Overall it is an introductory simulation to the bioprocess concepts behind wine fermentation, and could be improved in the future based on the learning objectives of the users.

4.4 AAT Enzyme in Other Yeast Strains

We were also interested in the structure of the AAT enzyme across different yeast strains. It was hypothesized that the structural variations could have caused the ester profile variations in commercial wine (fermented with commercial wine yeast strain EC1118) and lab wine sample (fermented with lab yeast strain S288c).

Despite there being only two point differences in the protein sequence alignment shown in Figure 15, the predicted protein structures of the ATF2 protein shown in Figure 16 did not superimpose with each other very well. This was partially because that the algorithm chosen in MODELLER to predict the protein structures was not optimizing loop structures. Therefore, it can be seen in Figure 16 that a lot of the alpha helices and beta pleated sheets had similar length and positions, but cannot superimpose very well due to

various loop structures. On the other hand, MODELLER makes protein structure predictions based on a template structure homologous to the target unknown protein structure (MODELLER, 2016). The homolog template found through PMP had 18% identity comparing to the target protein structure (ATF2). A good template usually has a percent identity higher than or equal to 30%, and the twilight zone for template search lies between 20% identity and 30% identity. The low percent identity offered by the template could be the other reason contributing to the inaccuracy of the predicted ATF2 models. However, from the superimposition figures with the two point differences highlighted (Figure 17 & 18), it can be seen that the protein had different secondary structures at the amino acid residue mismatch locations. The amino acid residue point differences could suggest potential structural differences between the ATF2 structures of the two yeast strains (EC1118 and S288c), which provided a potential cause of ester profile variations between the wine fermented by the two strains, respectively.

We were able to connect the biotechnology involved in wine fermentation with the bioprocess virtual visualization through this project. The modeling approach provided support to the theoretical foundation of wine fermentation industry, while the wine production approach provided insight on the variations between the customer perception of wine aroma and the scientific analysis results.

5. CONCLUSIONS AND FUTURE STEPS

Our research investigating the influencing factors of ester aroma profile in wine encompassed a broad group of topics. The wine production approach suggested wine fermentation conditions with potential to enhance the ester profile in wine aroma. The bioinformatics approach to investigate the structure of the AAT protein suggested that the structure of the AAT enzyme could be the key to the altered ester profile in different alcoholic beverages. The NetLogo simulation of the wine fermentation process suggested that the fermentation process generally follows the theoretical biochemical pathway, but the actual amount of ethanol and esters being produced could be altered easily with the change of fermentation conditions such as temperature and molecular interactions with yeast cells.

This project could step further in several aspects in the future. Firstly, the wine production approach should be replicated on grape must-based wine fermentation, so that the product can be evaluated not only on the aroma, but also on its color, content, and taste. The assays evaluating the transcription level of the ATF2 gene should be replicated by taking several yeast samples from the same fermentation flasks, as well as samples from replication flasks to get statistically reasonable results. Secondly, to evaluate the ATF2 gene expression in the translational level, a western blot specifically targeting the AAT enzyme should be done to provide more direct evidence of ATF2 expression level. Thirdly, the GC-MS analysis should be done immediately after taking the samples from the flasks to minimize the escape or degradation of volatile aromatic compounds from the samples.

Furthermore, to obtain a better prediction of the AAT enzyme structure, a continuous effort should be made to look for a better homologous template for the enzyme.

The wine fermentation simulation could also be modified to more closely match the teaching objectives of the Wine Research Center of University of Nova Gorica, when implementing and incorporating the simulation to their curriculum.

REFERENCES

Altschul, S. F., Maden, T. L., Schaffer, A. A., Zhang J., Zhang, Z., Miller, W., & Lipman D. J. (1997). Gapped BLAST and PSI-BLAST: a new generation of protein database search programs. Nucleic Acids Research, 25(17), 3389-3402.

Beekwilder J., van der Meer I. M., Sibbesen O., Broekgaarden M., Qvist, I., Mikkelsen, J. D., & Hall, R. D. (2007). Microbial production of natural raspberry ketone. *Biotechnology Journal*, 2(10), 1270-1279. DOI: 10.1002/biot.200700076

DiWineTaste. (2006). Making wine: grape harvest. *DiWineTaste.* Retrieved from: http://www.diwinetaste.com/dwt/en2006106.php

Fiser A., Sali A. (2003). Modeller: generation and refinement of homology-based protein structure models. Meth. Enzymol. 374: 461–91.

Frank, M. E., & Hettinger T. P. (2005). What the tongue tells the brain about taste. *Chemical Senses*, 30(suppl 1), i68-i69. http://chemse.oxfordjournals.org/content/30/suppl_1/i68.full

Grob, R. L., & Barry, E. F. (2004). *Modern Practice of Gas Chromatography*. Hoboken, NJ: John Wiley & Sons, Inc.

Huang, C. C., Couch, G. S., Pettersen, E. F., & Ferrin, T. E. (1996). Chimera: an extensible molecular modeling application constructed using standard components. In Pacific symposium on biocomputing (Vol. 1, No. 724, pp. 1519-1523).

Jackson, R. S. (2002). Wine tasting: a professional handbook. Waltham, Massachusetts: Academic Press.

Jia, M. (2016). Characterizing Impact of Initial Conditions on Fermentation in Two New Grape Wines. Undergraduate Major Qualifying Project. Worcester Polytechnic Institute.

Jimenez-Marti, E., Aranda A., Mendes-Ferreira, A., Mendes-Faia, A., & li del Olmo, M. (2007). The nature of the nitrogen source added to nitrogen depleted vinifications conducted by a Saccharomyces cerevisiae strain in synthetic must affects gene expression and the levels of several volatile compounds. *Antonie van Leeuwenhoek*, 92, 61-75. DOI: 10.1007/s10482-006-9135-1

Kodur, S. (2011). Effects of juice pH and potassium on juice and wine quality, and regulation of potassium in grapevines through rootstocks (Vitis): a short review. *Vitis*, 50(1), 1-6.

Owen, J. (2011). Earliest known winery found in Armenian caves. *National Geographic News.* Retrieved from: http://news.nationalgeographic.com/news/2011/01/110111-oldest-wine-press-making-winery-armenia-science-ucla/

Pieper, U., Eswar, N., Braberg, H., Madhusudhan, M. S., Davis, F. P., Stuart, A. C., . . . Sali, A. (2004). MODBASE, a database of annotated comparative protein structure models, and associated resources. *Nucleic Acids Research,* 32: 217 – 222.

Pires, E.J., Teixeira, J.A., Branyik, T., & Vicente, A.A. (2014). Yeast: the soul of beer's aroma – a review of flavor active esters and higher alcohols produced by the brewing yeast. Applied Microbiology Biotechnology. 98, 1937 – 1949. DOI: 10.1007/s00253-013-5470-0

Plumpton College. (2015). Managing the alcoholic fermentation. *Wineskills*. Retrieved from: http://www.wineskills.co.uk/winemaking/winemaking-knowledge-base/managing-alcoholic-fermentation

Promega Corporation. (2015). What percentage agarose is needed to sufficiently resolve my DNA sample? *Pubhub*. Retrieved from: https://worldwide.promega.com/resources/pubhub/enotes/what-percentage-agarose-is-needed-to-sufficiently-resolve-my-dna-sample/?activeTab=0

Railsback, S. F., & Grimm, V. (2012). Agent-based and indivicual-based modeling. Princeton, NJ: Princeton University Press.

Rapp A. & Mandery H. (1986). Wine Aroma. *Experientia*, 42(8), 873-884. DOI: 10.1007/BF01941764

Robinson, J., & Harding J. (Eds.) (2015). The Oxford Companion of Wine. Oxford, UK: Oxford University Press.

Rotter, B. (2008). Yeast Strains. *Improved Winemaking*. Retrieved from: http://www.brsquared.org/wine/CalcInfo/yeasts.htm#T73

Saccharomyces Genome Databases (SGD). (2016). Genome Browser [data file] Retrieved from: http://browse.yeastgenome.org

‘

Swiegers, J. H., Bartowsky, E. J., Henschke, P. A., & Pretorius, I. S. (2005). Yeast and bacterial modulation of wine aroma and flavour. *Australian Journal of Grape and Wine Research*, 11(2), 139-173. DOI: 10.1111/j.1755-0238.2005.tb00285.x

Tronchoni, J., Gamero, A., Arroyo-Lopez, F. N., Barrio E., & Querol, A. (2009). Differences in the glucose and fructose consumption profiles in diverse Saccharomyces wine species and their hybrids during grape juice fermentation. *International Journal of Food Microbiology*, 134(3), 237-243. DOI: 10.1016/j.ijfoodmicro.2009.07.004

Viana, T., Loureiro-Dias, M. C., & Prista C. (2014). Efficient fermentation of an improved synthetic grape must by enological and laboratory strain Saccharomyces cerevisiae. *AMB Express*. Retrieved from: http://www.ncbi.nlm.nih.gov/pmc/articles/PMC4052690/

Voet, D., Voet, J.G., & Pratt, C.W. (2013). Fundamentals of biochemistry: Life at the molecular level. Hoboken, NJ: Wiley.

Wines of Germany. (2003). Must weights. *Wines of Germany*. Retrieved from: http://www.germanwines.de/knowledge/quality-standards/must-weights/

Whyeast Laboritories, Inc. (2006). What is yeast. Retrieved from: https://www.wyeastlab.com/he-yeast-fundamentals.cfm

APPENDIX A

Wine Research Center/University of Nova Gorica

Sensory Analysis/Project: WPI WINE MQP

Date: 08.12.2015/Location: Lantheri Mansion/Testing Group: 1 2 3 4 5

Flavor/Smell	**<- Less More->**
Persistence of flavor	
Intensity of flavor	
Quality of flavor	
Fresh fruit (citrous)	
Apple, pear	
Banana	
Berries, soft red fruits like strawberry/cherry	
Flower-like	
Spices	
Sweetish, honey	
Unpleasant (nail polish, soap, …)	
Overall Impression	

APPENDIX B

The optical density (OD) reading of the standard bovine serum albumin (BSA) solution and the samples can be seen in Table 6 below.

Table 7: Bradford Assay BSA Standard OD Reading

Sample	OD Reading (A)
BSA Standard 2 mg/mL	1.150
BSA Standard 1 mg/mL	0.845
BSA Standard 0.5 mg/mL	0.477
BSA Standard 0.25 mg/mL	0.164
BSA Standard 0.125 mg/mL	0.057
1	0.046
2	0.014
3	0.016
4	0.029
5	0.048
6	0.033
7	0.059
8	0.039
9	0.035

The OD readings lower than 1A for the BSA standard samples were plotted on a scatter plot and a linear progression was generated. The plot and the linear progression can be seen in Figure 24 below.

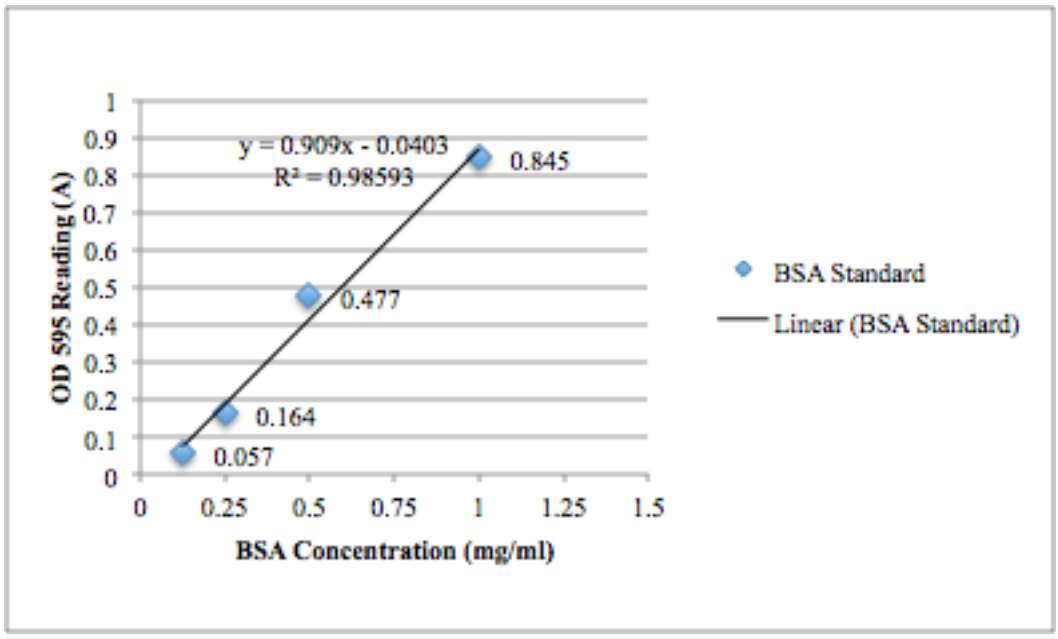

Figure 26: Bradford Assay Standard Curve

It can be seen in Figure 16 that the equation for the linear progression of the BSA standard is:

$y = 0.909x - 0.0403$ (1)

The OD readings of the yeast protein extract samples were then set as y values in Equation 1 above and the protein concentration value x was calculated as the following sample calculation:

When $y = 0.048$ (Sample 5 OD Reading),

$0.048 = 0.909x - 0.0403$

$x = 0.097$ mg/ml

APPENDIX C

Wine Simulation User Guide

- Wine View

WHAT IS IT?

This model demonstrates the molecular interaction in wine fermentation and provides insight on the production level of ethanol and esters in wine.

HOW IT WORKS

The cold soak step of the simulation is majorly controlled by the cold soak temperature. For red wine, the cold soak temperature should be lower than or equal to 10 degree Celsius. If the cold soak temperature is set in this range, the background color will advance into the red wine color. Otherwise the background color will advance into either yellowish white (white wine color), or white (representing transparent solution).

The fermentation model has four agents: yeast cells (white, big, egg shaped, one agent representing 1 OD unit of yeast cells), glucose (yellow, small, dot, one agent representing 1 mmol of glucose), ethanol (orange, small, dot, one agent representing 1 mmol of ethanol), and ester (blue, small, dot, one agent representing 1 mmol of ester). The glucose diffuse in the environment and collide with the stationary yeast cells at the bottom of the "fermentation container". Upon collision, the glucose disappear and generate two transparent pyruvate agents (since pyruvates only exist inside of the yeast cells but to follow the biochemical pathways the pyruvates are set to be transparent and cannot be seen by the users). The pyruvate agents then diffuse in the wine and collide with yeast cells. Each collision has a 1:90 chance to create an ester agent. Otherwise the collision will create an ethanol agent and delete the pyruvate agent. This chance disparity is to simulate the abundance disparity between the alcohol dehydrogenase (ADH) and the alcohol acetyltranseferase (AAT) in yeast cell. The simulation stops when the level of sugar in the environment reaches 10 mmol.

The biochemical pathway applied in this simulation:

Glucose + 2 NAD+ + 2 ADP + Pi –glycolysis–> 2 Pyruvate + 2 NADH + 2 ATP + 2 H2O + 2 H+

Pyruvate –> Acetylaldehyde –ADH–> Ethanol

Pyruvate –> Acetyl-CoA –AAT–> Esters

HOW TO USE IT

First set a temperature for the cold soak process. Click Cold Soak! and then click Cold Soak Timer to start cold soaking. The cold soak process will stop when the wine background reaches the optimum color. However, the timer can be stopped at any time you would like just by clicking on the Cold Soak Timer again. If you would like to reset the color of the wine, click on "Start" button.

Then set a temperature for the fermentation process. This will dictate the yeast growth rate as well as the speed of the molecule movement in wine. Then "Set Up Fermentation" to have all the agents in the environment. Then "Ferment!".

THINGS TO NOTICE

The legend on the left lower corner shows what agent represents what molecule. The monitors under the buttons shows the current amount of molecules in the unit that they are commonly measured.

THINGS TO TRY

As mentioned in the previous descriptions, the cold soak temperature slider controls the final color of the wine; the fermentation temperature slider controls the speed of the yeast growth as well as the speed of molecule movements. Users are encouraged to try out different temperatures to discover how temperature influences the wine fermentation process.

RELATED MODELS

This model is developed at the same time with the yeast view fermentation model, which demonstrates the wine fermentation process within the yeast cell – interactions between the chemicals and the yeast enzymes.

CREDITS AND REFERENCES

Credit to the Major Qualifying Project "Yeast and Wine Aroma", Tete Zhang, Class of 2016, Department of Bioinformatics and Computational Biology, Worcester Polytechnic Institute, 2016.

- Yeast View

WHAT IS IT?

This model demonstrates the wine fermentation process in a cellular level, simulating the molecule-enzyme interactions inside of a yeast cell.

HOW IT WORKS

The cold soak step of the simulation is majorly controlled by the cold soak temperature. For red wine, the cold soak temperature should be lower than or equal to 10 degree Celsius. If the cold soak temperature is set in this range, the background color will advance into the red wine color. Otherwise the background color will advance into either yellowish white (white wine color), or white (representing transparent solution).

The fermentation model has seven agents: sugar transporters (yellow square), glucose (yellow, smalldot), pyruvate (green, small dot), ethanol (orange, small dot), ester (blue, small dot), glycolysis enzyme complex (green circle), alcohol dehydrogenase (ADH, orange circle), and alcohol acetyltransferase (AAT, blue circle). The glucose diffuse in the environment and collide with the sugar transporters to get in and out of the yeast cell. Upon collision of glucose and glycolysis enzyme complex, the glucose disappear and generate two pyruvate agents. The pyruvate agents then diffuse in the cell and collide with either ADHs or AATs. Each collision with ADHs will kill the pyruvate agent and generate an ethanol agent. Each collision with AATs will kill the pyruvate agent but only generate an ester agent in a 1:10 chance. This is to ensure the enzyme abundance disparity in the real yeast cells, however since showing 1 AAT and 90 ADHs is not visually welcoming, the grow by chance algorithm was introduced.

The biochemical pathway applied in this simulation:

Glucose + 2 NAD+ + 2 ADP + Pi –glycolysis–> 2 Pyruvate + 2 NADH + 2 ATP + 2 H2O + 2 H+

Pyruvate –> Acetylaldehyde –ADH–> Ethanol

Pyruvate –> Acetyl-CoA –AAT–> Esters

HOW TO USE IT

First set a temperature for the cold soak process. Click Cold Soak! and then click Cold Soak Timer to start cold soaking. The cold soak process will stop when the wine background reaches the optimum color. However, the timer can be stopped at any time you would like just by clicking on the Cold Soak Timer again. If you would like to reset the color of the wine, click on “Start” button.

Then set a temperature for the fermentation process. This will dictate the yeast growth rate as well as the speed of the molecule movement in wine. Then “Set Up Fermentation” to have all the agents in the environment. Then “Ferment!”.

THINGS TO NOTICE

The legend on the left lower corner shows what agent represents what molecule. The monitors under the buttons shows the current amount of molecules in the environment.

THINGS TO TRY

As mentioned in the previous descriptions, the cold soak temperature slider controls the final color of the wine; the fermentation temperature slider controls the speed of molecule movements. Users are encouraged to try out different temperatures to discover how temperature influences the wine fermentation process.

If the "Overexpress-AATs" switch is on before setting up the fermentation, the amount of ester producing enzymes (alcohol acetyltransferase, AAT) will be made 10 times more than when the switch is off, giving the pyruvate agents more chances to interact with the AATs and therefore make more ester products.

If the "Reaction-Monitor" switch is on, the sugar molecules will not disappear after colliding with the glycolysis enzyme complex, but turns into dark brown and can no longer interact with other agents in the environment. This is to give the users a clearer demonstration of the biochemical pathway, showing the life path of the sugar molecules, as well as the production of the pyruvate agents.

RELATED MODELS

This model is developed the same time as the wine view of wine fermentation process, which demonstrates the interactions between chemicals and the yeast cells in a more detailed perspective, where users can see the chemical reactions happen.

CREDITS AND REFERENCES

Credit to the Major Qualifying Project "Yeast and Wine Aroma", Tete Zhang, Class of 2016, Department of Bioinformatics and Computational Biology, Worcester Polytechnic Institute, 2016.